THE VIBRO-IMPACT RESPONSE OF HEAT EXCHANGER U-BEND TUBES WITH FLAT BAR SUPPORTS

THE VIBRO-IMPACT RESPONSE OF HEAT EXCHANGER U-BEND TUBES WITH FLAT BAR SUPPORTS

by

Metin Yetisir, B.Sc. (Mech. Eng.)

A thesis

Submitted to the School of Graduate Studies

in Partial Fulfilment of the Requirements

for the degree

Master of Engineering

McMaster University

October 1985

MASTER OF ENGINEERING — McMASTER UNIVERSITY

(Mechanical Engineering) — Hamilton, Ontario

TITLE: The vibro-impact response of heat exchanger U-bend tubes with flat bar supports

AUTHOR: Metin Yetisir, B.Sc. (Mech. Eng.) (Middle East Technical University, Ankara, Turkey)

SUPERVISOR: Dr. D.S. Weaver

NUMBER OF PAGES: xi, 80

ABSTRACT

A theoretical study has been conducted to investigate the effect of flat bar supports on the dynamic response of a heat exchanger U-tube. The tube is modelled using three dimensional, six degrees of freedom per node straight beam finite elements. A new method, the stiffness method, is introduced to compute the impact forces at the supports. It is compared with the previously used external force method. Modal analysis is employed to investigate the modal energy dissipation in the higher modes. Time response of the U-tube is analysed using a Fast Fourier Transform algorithm. The effects of clearance, excitation magnitude, and mode coupling through friction at the supports are investigated.

ACKNOWLEDGEMENTS

The author wishes to express his sincere gratitude and indebtedness to his supervisor Dr. D.S. Weaver. His constant encouragement and advice were invaluable throughout the course of this study.

The author is also grateful to Mr. Ralph Harris for the use of his computer software and for his competent assistance. The willing cooperation of Mr. Robert Lafflamme, Mr. Kemal Berkkan, Mr. Peter Scott and Miss Elizabeth Brown is gratefully acknowledged.

Thanks are due to the Engineering Word Processing Centre for typing the manuscript.

TABLE OF CONTENTS

TABLE OF CONTENTS (continued)

LIST OF TABLES

LIST OF FIGURES

LIST OF FIGURES (continued)

NOMENCLATURE

$[C]$	System damping matrix
c_r	Radial clearance between the heat exchanger tube and the flatbar support
d_i	Inner diameter of the heat exchanger tube
d_o	Outer diameter of the heat exchanger tube
E	Modulus of elasticity
F_{exc}	Excitation force
F_{spr}	Spring force
F_{dmp}	Damping force
F_f	Friction force
F_{imp}	Impact force
F_{fus}	Friction force along $\mathbf{u}_s$
F_{fub}	Friction force along $\mathbf{u}_b$
$\mathbf{i},\mathbf{j},\mathbf{k}$	Unit vectors along the x,y, and z axes respectively
$[K]$	System stiffness matrix
$[K_m]$	Modified system stiffness matrix
$[k_i]$	Contribution of the i'th support to the system stiffness matrix
k_{sp}	Stiffness of the support
$[M]$	System mass matrix
m_a	Added mass
$\mathbf{n}_s$	Unit normal vector of the support
n_{xs}	Direction Cosine of $\mathbf{n}_s$ in the x direction
n_{ys}	Direction Cosine of $\mathbf{n}_s$ in the y direction
n_{zs}	Direction Cosine of $\mathbf{n}_s$ in the z direction
$\mathbf{n}_{sm}$	Modified unit vector of the support

$\{q\}$	Displacement array in generalized coordinates
$\{r\}$	Displacement array in cartesian coordinates
R	Outer radius of the tube
r_{sup}	Total displacement toward the support
TQ	Torque/bending moment introduced by F_f
t_c	Contact duration
$\mathbf{u}_b$	Unit vector along the tube exis at the support
$\mathbf{u}_s$	A unit vector on the flat bar surface
$\mathbf{v}$	Velocity vector
v_{us}	Velocity component along $\mathbf{u}_s$
v_{ub}	Velocity component along $\mathbf{u}_b$
x_i,y_i,z_i	x,y, and z coordinates of node i
α	Material damping constant
δ	Deflection of the support
ρ_b	Density of the beam
ρ_{sur}	Density of the surrounding medium
ξ_i	Critical damping of the i'th mode
μ	Coefficient of friction
ν	Poisson's ratio
ϕ_i	Mode shape of i'th mode
$[\Phi]$	The transformation matrix from cartesian coordinates to generalized coordinates
ω_i	Frequency of the i'th mode

CHAPTER 1

INTRODUCTION

Tube and shell heat exchangers such as steam generators, heat exchangers, moderator coolers and condensers are integral parts of nuclear power stations. In this type of heat exchanger (Figure 1.1), one fluid flows inside the tubes while the another fluid is forced through the shell and over the outside of the tubes. The trend in modern heat exchanger design is to increase flow rates and to impose minimum structural constraints for higher efficiency. The former increases the heat transfer rate whereas the latter decreases the pressure drop. These requirements might lead to problems due to flow induced vibrations (FIV). The only practical way to reduce the vibration amplitude for a given flow velocity, is to alter the structure design by using antivibration supports. The heat exchanger U-tube supports need special designs due to the curvature. Weaver and Schneider [2] reported a variety of support geometries for heat exchanger U-tubes (Figure 1.2). They investigated the effectiveness of flat bar supports.

1.1 EXCITATION MECHANISMS

Paidoussis [1] broadly classifies the types of flow which might cause vibration problems as, (i) cross flow, (ii) internal axial flow, (iii) external axial flow, and (iv) annular or leakage flow. In heat exchangers, the most important among them is cross flow. Although, the excitation mechanisms are not fully understood, four principal mechanisms have been identified as possible sources of the cross-flow induced vibration :

(1) Vortex shedding

(2) Turbulent buffetting

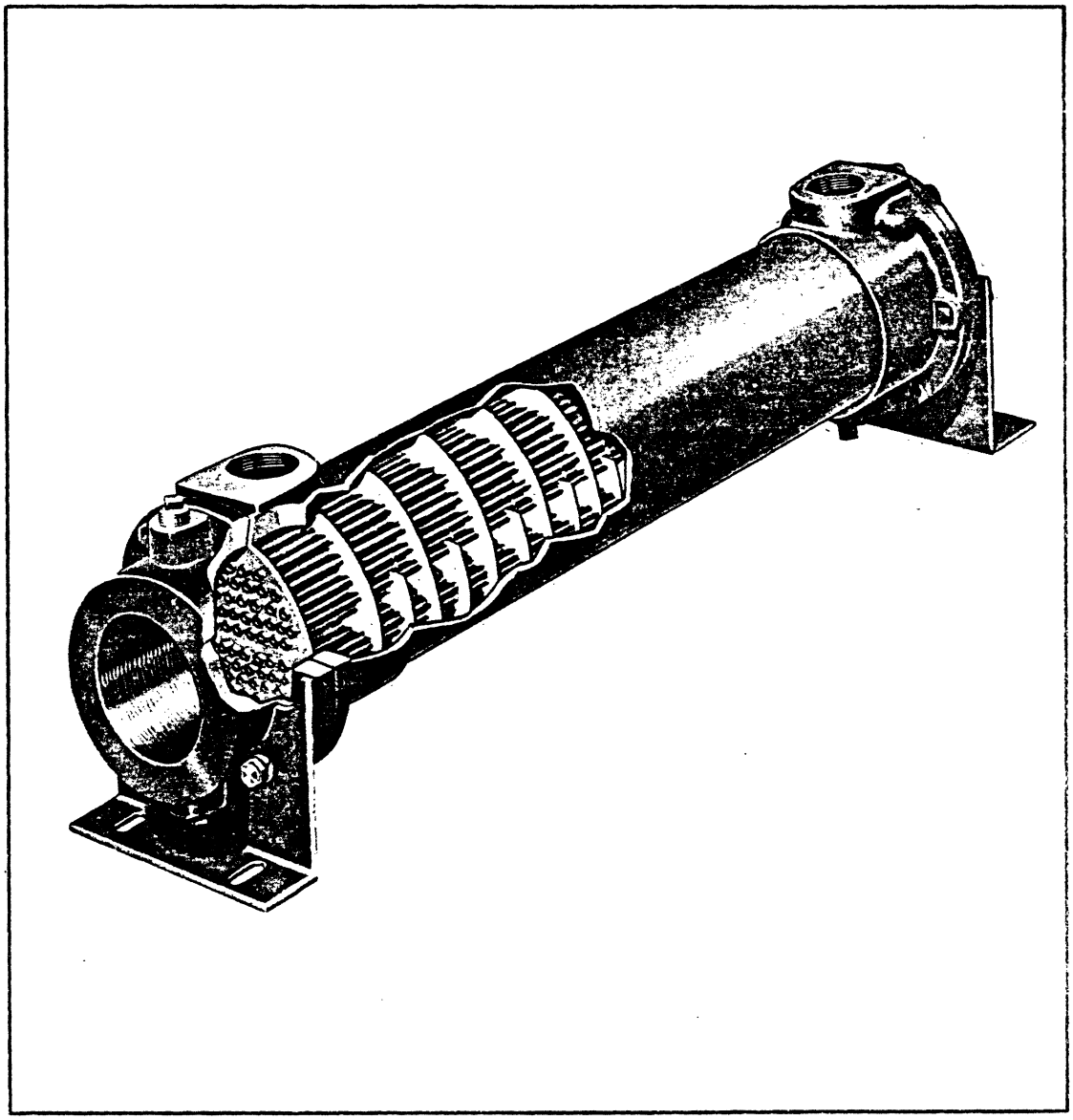

Figure 1.1 Tube and shell heat exchanger (from [23]).

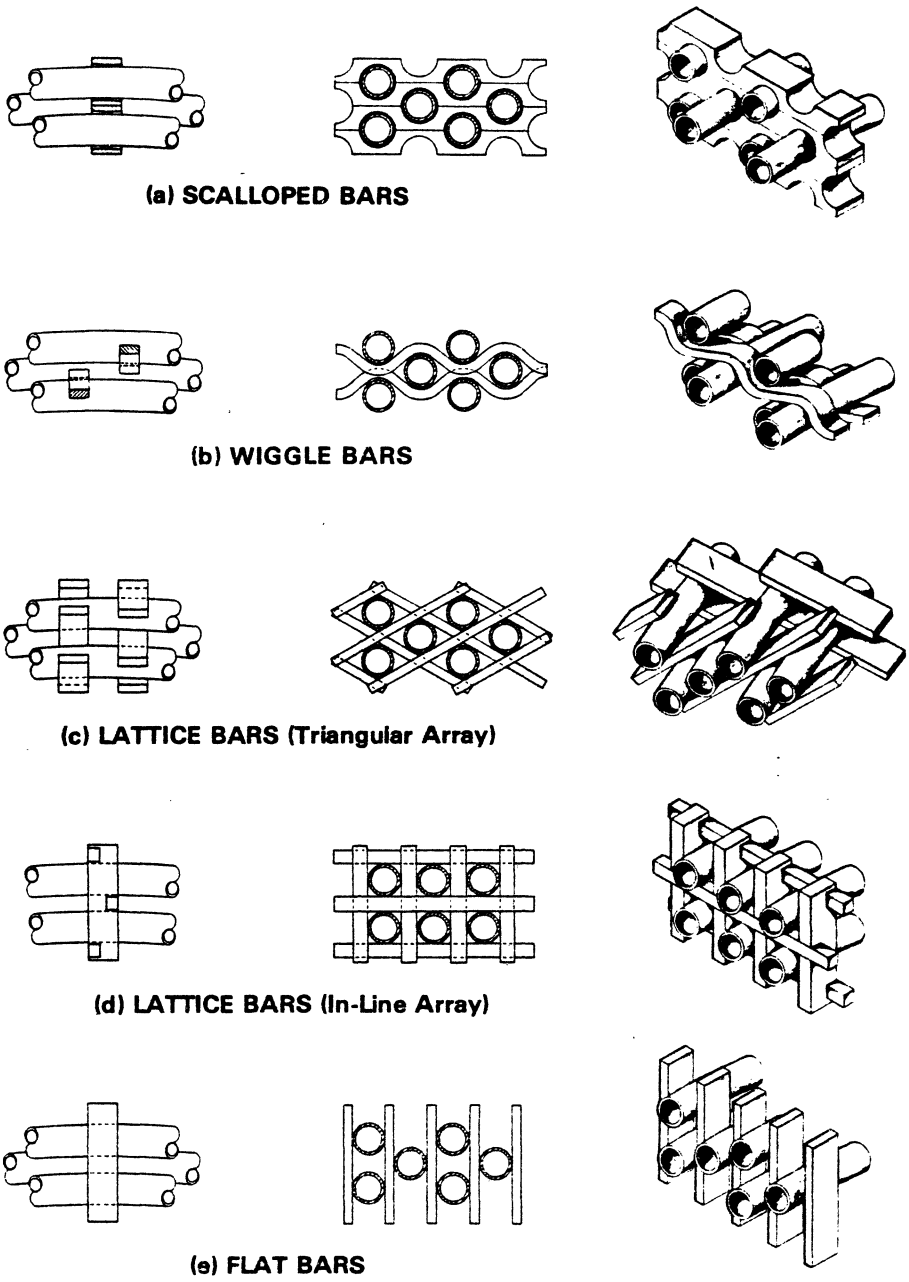

Figure 1.2 Various U-tube support configurations (from [2]).

(3) Fluidelastic instability

(4) Acoustic resonance

Depending on the tube vibration levels, heat exchanger tubes may fail either shortly after they are put into operation or after several years of service. In the former case, the cause is mainly due to fluidelastic instability. In the latter case, the interaction between the tube and the cross-flow is relatively weak, but continuous impacting and rubbing causes fretting wear and/or fatigue failure. Although the data shows considerable scatter, there are sufficient data in the literature for conventional heat exchangers to avoid conditions leading to short term heat exchanger tube failure due to fluidelastic instability. However, small amplitude vibrations caused by turbulent buffetting and vortex shedding might lead to unpredictable long term fretting failures. Fretting wear is a combination of the adhesive, abrasive, and corrosive mechanisms linked with the appearance of surface fatigue [23]. The prevention of slip between contacting surfaces prevents fretting wear. Thus an increase in the coefficient of friction could suppress fretting wear if the oscillation was also eliminated. However, it may encourage fretting wear if it does not stop the oscillatory motion. The remedy often lies in reducing the tangential force [23]. This can be done by imposing a soft material which might absorb tangential displacements and eliminate slip. In general, lubrication would also tend to reduce fretting wear. Unfortunately, neither lubrication nor soft material (i.e. rubber gaskets) are practical solutions for the fretting wear of heat exchanger tubes. Predictions of such failures is not easy, however there has been some excellent research done in this area in the last decade.

1.2 PREVIOUS WORK ON TUBE-SUPPORT INTERACTION

In order to accomodate tube motions due to thermal expansion and unavoidable manufacturing tolerances, there is usually clearance between tubes and supports. Therefore,

tube-support impacting always exists. Due to the clearance, the tube-support impacting is nonlinear and difficult to handle with analytical techniques. Some attempts [3]-[5] have been made in order to understand analytically the fundamental mechanisms of beam-support interaction. Piecewise linear solutions have been reported for very simple beam geometries with limited degrees of freedom. i.e. a pinned-pinned beam with a support at the middle [3,4], and a cantilever beam with a support at the tip [5].

The application of the Finite Element Method has enabled researchers to investigate the tube-support interaction in three dimensions for almost any kind of beam geometry. Bohm and Nahavandi [6], employed the finite element method to study the dynamics of reactor internals, including the effect of support impacts. Elliot [7] did similar work for predicting the natural frequencies of multi-spanned tubes with curved sections and the dynamic response of a vibratory tube impacting a support. Although he achieved reasonable agreement with the experimental data, his program could not handle a large number of finite elements due to inefficient global matrix constructions. Rogers and Pick [8] modified and extended Elliot's approach and reported good agreement between calculated and experimental values of RMS impact force levels. They also employed the modal superposition method in their dynamic analysis to reduce the computing time. Modal analysis increases the efficiency of the computer program by reducing the half bandwidth of the global matrices and leaving out the unwanted modes. All of these authors used a linear spring model for the supports. They either assumed or experimentally measured the support stiffness. Shin et al. [9] used a nonlinear contact force-deflection relationship taking into account the contact geometry and material properties. Since, this relationship is derived for the elastic cylinder, but not for the tube, the stiffness values calculated by using this formula are about two orders of magnitude higher than the experimental one [8]. The reason for this discrepancy must be due to the ovalization effect which was not taken into account in the elastic cylinder model.

They did not employ the modal superposition, since they believed the higher modes were playing an important role and shouldn't be eliminated from the analysis.

Haslinger and Steininger [11] produced a set of data to investigate tube wearing. They are planning to correlate their theoretical results with the experimental wear data when the experimental data is available. Their wear-work parameter, $F_{imp}*x_s$ might be found to be linearly proportional to the wear rate, if the Archard's fretting wear equation, $V(t) = kF_{imp}(t)\, x_s(t)$, is valid for the heat exchanger tube fretting, where V(t) is the material removal rate, k is a constant, F_{imp} is the impact force, and x_s is the sliding distance. Axisa et al. [12] report linearized behaviour of the non-linear tube support impacting for high excitation levels. Their results show that the effect of clearance on the RMS impact force is rather small. They obtained their results in terms of "Equivalent Impact Force", EIF, which is the ensembled average value of the RMS impact force in one characteristic cycle. Although they reported good agreement between experimental and theoretical results, the concept of EIF may not be applicable to the systems which don't have a definite single characteristic cycle.

Some experimental research has also been reported on the tube-support interaction. These studies [14,15] attempted to predict fretting failures by correlating the RMS impact forces with the fretting wear rates. Ko [14] reported that the rate of wear is linear with time and with the RMS impact force levels and is independent of the frequency. He also reported that the clearance has a significant effect on the wear rate. Roger's [8] experience with Ko's ring, however, leads him to doubt Ko's experimental results although Ko's qualitative results should still be valid. Similar qualitative results were also reported by Blevins [16].

All of these studies have considered solid support plates perforated with holes for the tubes to pass through. Such supports are not suitable for U-bend tubes and the various alternatives (Figure 1.2) are discussed by Weaver and Schneider [2]. Among these designs,

flat bars are the simplest ones, yet apparently very effective in practical use. They allow thermal expansion which might be a problem in other support designs and also provide a very open structure for the flow. Build-up of deposits is minimal and flexibility is good for differential tube motions [2]. Although they provide little obvious support to in-plane tube motions, they have been demonstrated as being very effective anti-vibration supports.

1.3 STATEMENT OF THE PROBLEM

Weaver and Schneider [2] experimentally investigated the FIV characteristics of the flat bar supports. They reported that flat bars created nodal points for the U-bend tubes even though there is not rigid in-plane support provided that the support clearances were kept sufficiently small. As additional sets of flat bars were added, successively higher out-of-plane modes were excited by the flow. No in-plane instability was observed, even when the flow velocity exceeded three times that expected to create fluidelastic instability in the first in-plane mode. The reason for this behaviour is not understood. Clearly, there is a need for additional research on the fundamental aspects of tube-support interaction.

The purpose of the present theoretical study was to examine the structural dynamics aspects of heat exchanger tubes with flat bar supports. Of special interest were the effects of friction at the supports, damping in the higher modes excited by tube impacting, coupling between in-plane and out-of-plane modes and support clearance. It was thought that an understanding of dynamic response characteristics of the tube-support interaction will be gained through this study.

1.4 BRIEF SUMMARY OF THESIS

The FEM analysis of the beam-support interaction is discussed in the second chapter. The selection of the beam element and the numerical integration scheme are

explained. The damping model and the technique of determining significant modes in energy dissipation are also presented. The uncoupled equations of motion are obtained by means of modal analysis. Mode coupling of the U-bend tubes and the mechanisms introduced due to flat bar supports are explained. A new method to determine the impact forces is introduced. It is compared with the external force method which has been used by other researchers.

In Chapter three, the mathematical modelling of the tube-support interaction is given. Equations are derived for the general case where the flat bars are not in the plane of the U-bend. Modelling of the flat bars and the simplifying assumptions are discussed. Calculations of the friction force, the damping force and the moments are presented.

Results and a subsequent discussion are given in Chapter four. A parametric study was carried out for a one and two dimensional cantilever beam. One heat exchanger U-bend tube with flat bar supports at the apex is investigated in three dimensions. The effect of the higher modes are found to be not as important as had been thought. A Fast Fourier Transform on the tube response is performed to examine its frequency content. The effects of the excitation level, the mode coupling through friction at the flat bar supports, and the clearance are presented and discussed.

Conclusions of the present study are presented in Chapter five. It is found that the mode coupling and the damping in the higher modes are not significant in the stable range. Further research is necessary to fully understand the effectiveness of the flat bars.

CHAPTER 2

F.E.M. ANALYSIS OF TUBE-SUPPORT INTERACTION

A beam FEM program, was developed to investigate the response of heat exchanger tubes when they impact flat bar supports. It was suspected that higher order modes might be very important due to impacting. A model was developed to determine the effective modes. A new method, the stiffness method, was introduced to calculate the impact forces and was compared with the external force method.

2.1 THE EQUATIONS OF MOTION FOR THE COMPLETE SYSTEM

The equations of motion of the discretized system is given as:

$$[M]\{\ddot{r}(t)\} + [C]\{\dot{r}(t)\} + [K]\{r(t)\} = \{F(t)\} \tag{2.1}$$

where

[M] is the system mass matrix

[C] is the system damping matrix

[K] is the system stiffness matrix

{r(t)} is the modal displacement array

{F(t)} is the external force vector.

Heat exchanger tubes can be considered as continuous beams with intermittent supports. The dynamic response of such structures can successfully be found by using beam finite elements. Beam finite elements are the simplest finite elements, yet the accuracy is satisfactory with a very few number of elements in many cases. It has been concluded [18] that the simple McCalley element is the most suitable one for general purpose applications. A correctly chosen higher order element may perform better, but it is not always easy to

determine which element is the most suitable for a particular application. In the case of an improper selection, the accuracy may be poorer than with the simple element.

To investigate the energy transfer from one mode to another by means of mode coupling and impacting, a 6 degrees of freedom/node beam element was selected (Figure 2.1). This permits the effect of torsion and bending to be included. This element includes all possible motions in three dimensions, namely, three translational degrees of freedom and three rotational degrees of freedom.

2.1.1 INERTIA PROPERTIES

There are two types of mass matrices; the first being consistent and full, the second being lumped and diagonal. Consistent mass matrices usually give more accurate frequencies for flexural members like beams and shells [20]. This advantage, however, becomes small whenever the wavelength of the mode spans five or more elements. The consistent mass approach usually overestimates the frequencies whereas the lumped mass approach underestimates them [21]. Although the lumped mass model decreases the computation time and hence the cost, the consistent mass matrix approach will be used in this research because of the higher accuracy in predicting eigenvalues. The consistent mass matrix given by Przemieniecki [19] is shown in Figure 2.2. The added mass effect can also be included by calculating the added mass with the formula given below. It is included in the global mass matrix as lumped masses.

$$m_a = \rho_{sur} \pi R^2 l_e$$

where ρ_{sur} is the density of the surrounding.

R is the outer radius of the tube

l_e is the length of the finite beam element

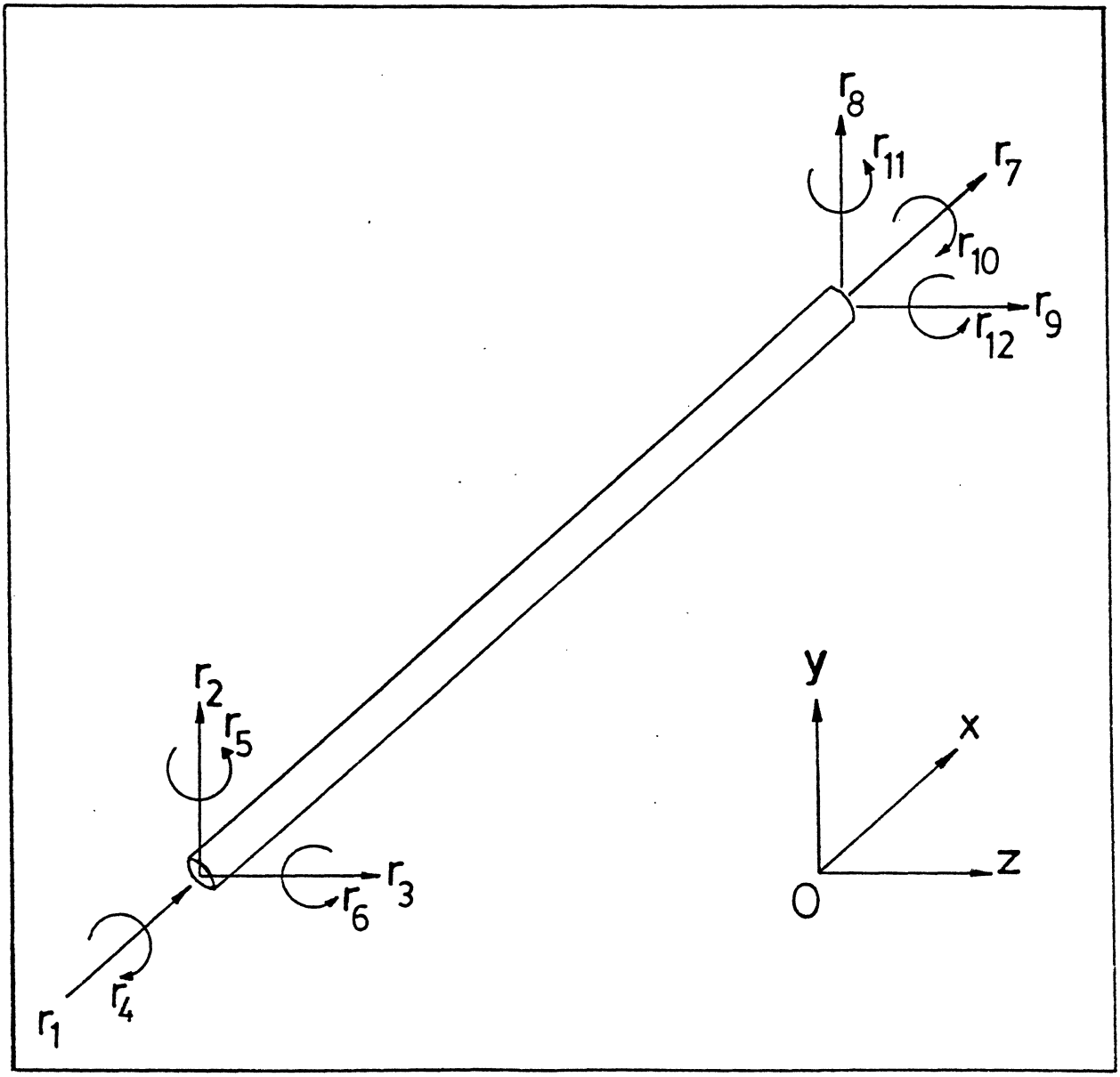

Figure 2.1 6 d.o.f./node straight beam element.

$$[M] = \rho A l$$

$\frac{1}{3}$												
0	$\frac{13}{35}+\frac{6I_z}{5Al^2}$											
0	0	$\frac{13}{35}+\frac{6I_y}{5Al^2}$										
0	0	0	$\frac{J_x}{3A}$									
0	0	$-\frac{11l}{210}-\frac{I_y}{10Al}$	0	$\frac{l^2}{105}+\frac{2I_y}{15A}$								
0	$\frac{11l}{210}+\frac{I_z}{10Al}$	0	0	0	$\frac{l^2}{105}+\frac{2I_z}{15A}$							
$\frac{1}{6}$	0	0	0	0	0	$\frac{1}{3}$						
0	$\frac{9}{70}-\frac{6I_z}{5Al^2}$	0	0	0	$\frac{13l}{420}-\frac{I_z}{10Al}$	0	$\frac{13}{35}+\frac{6I_z}{5Al^2}$					
0	0	$\frac{9}{70}-\frac{6I_y}{5Al^2}$	0	$-\frac{13l}{420}+\frac{I_y}{10Al}$	0	0	0	$\frac{13}{35}+\frac{6I_y}{5Al^2}$				
0	0	0	$\frac{J_x}{6A}$	0	0	0	0	0	$\frac{J_x}{3A}$			
0	0	$\frac{13l}{420}-\frac{I_y}{10Al}$	0	$-\frac{l^2}{140}-\frac{I_y}{30A}$	0	0	0	$\frac{11l}{210}-\frac{I_y}{10Al}$	0	$\frac{l^2}{105}+\frac{2I_y}{15A}$		
0	$-\frac{13l}{420}+\frac{I_z}{10Al}$	0	0	0	$-\frac{l^2}{140}-\frac{I_z}{30A}$	0	$-\frac{11l}{210}-\frac{I_z}{10Al}$	0	0	0	$\frac{l^2}{105}+\frac{2I_z}{15A}$	

Symmetric

Figure 2.2 Mass matrix for 6 d.o.f./node beam element (from [19]).

2.1.2 STIFFNESS PROPERTIES

Przemieniecki [19] gives the elemental stiffness matrix for the same element (Figure 2.3). The effect of shear is also included. The coefficients of shear to determine the shear area are given by Cowper [22] for various simple cross-sections.

2.1.3 DAMPING

In a vibrating system, damping may be encountered in the form of internal molecular friction (material damping), fluid resistance (fluid damping) and scraping-sliding-impacting motion (structural damping). Generally the mathematical description of these damping mechanisms is quite complex and not suitable for vibration analyses. Thus simplified damping models have been developed that in many cases have been found to be adequate in evaluating the system response. The viscous damping model is the one used in vibration analyses because of the simplicity of its mathematical manipulations. In this model the damping force is assumed to be proportional to the velocity. Structural damping is usually expressed in terms of viscous damping and then included in the mathematical model.

Heat exchanger tubes have combined material,structural and fluid damping. As a result, the total damping is a function of many variables and the literature on the damping of heat exchanger tubes with support clearance gives scattered wide ranging data. Although the critical damping range of 0.3%-1.0% [16] is typical, very high critical damping values (as high as 11% [9]) have been reported. The damping mechanism at the supports is not well understood, but the highly scattered data implies that structural damping due to tube-support impacting,sliding and rubbing has a significant effect on the total damping and hence on the vibration responses.The following qualitative results have been reported by many researchers[2,8,9,16,23]:

1. The equivalent viscous damping factor decreases in higher modes

$$\Phi_y = \frac{12EI_z}{GA_{s_y}l^2} = 24(1+\nu)\frac{A}{A_{s_y}}\left(\frac{r_z}{l}\right)^2$$

$$\Phi_z = \frac{12EI_y}{GA_{s_z}l^2} = 24(1+\nu)\frac{A}{A_{s_z}}\left(\frac{r_y}{l}\right)^2$$

$$[K] = \begin{bmatrix}
\frac{EA}{l} & & & & & & & & & & & \\
0 & \frac{12EI_z}{l^3(1+\Phi_y)} & & & & & & & & & & \\
0 & 0 & \frac{12EI_y}{l^3(1+\Phi_z)} & & & & & & & & & \\
0 & 0 & 0 & \frac{GJ}{l} & & & & & & & & \\
0 & 0 & \frac{-6EI_y}{l^2(1+\Phi_z)} & 0 & \frac{(4+\Phi_z)EI_y}{l(1+\Phi_z)} & & & & & & & \\
0 & \frac{6EI_z}{l^2(1+\Phi_y)} & 0 & 0 & 0 & \frac{(4+\Phi_y)EI_z}{l(1+\Phi_y)} & & & & & & \\
\frac{-EA}{l} & 0 & 0 & 0 & 0 & 0 & \frac{AE}{l} & & & & & \\
0 & \frac{-12EI_z}{l^3(1+\Phi_y)} & 0 & 0 & 0 & \frac{-6EI_z}{l^2(1+\Phi_y)} & 0 & \frac{12EI_z}{l^3(1+\Phi_y)} & & & & \\
0 & 0 & \frac{-12EI_y}{l^3(1+\Phi_z)} & 0 & \frac{6EI_y}{l^2(1+\Phi_z)} & 0 & 0 & 0 & \frac{12EI_y}{l^3(1+\Phi_z)} & & & \\
0 & 0 & 0 & \frac{-GJ}{l} & 0 & 0 & 0 & 0 & 0 & \frac{GJ}{l} & & \\
0 & 0 & \frac{-6EI_y}{l^2(1+\Phi_z)} & 0 & \frac{(2-\Phi_z)EI_y}{l(1+\Phi_z)} & 0 & 0 & 0 & \frac{6EI_y}{l^2(1+\Phi_z)} & 0 & \frac{(4+\Phi_z)EI_y}{l(1+\Phi_z)} & \\
0 & \frac{6EI_z}{l^2(1+\Phi_y)} & 0 & 0 & 0 & \frac{(2-\Phi_y)EI_z}{l(1+\Phi_y)} & 0 & \frac{-6EI_z}{l^2(1+\Phi_y)} & 0 & 0 & 0 & \frac{(4+\Phi_y)EI_z}{l(1+\Phi_y)}
\end{bmatrix}$$

Symmetric

Figure 2.3 Stiffness matrix for 6 d.o.f./node beam element (from [19]).

2. The equivalent viscous damping factor increases with increasing excitation force amplitude.

The material damping of a structure is a function of geometry, material properties and the mode shape. For example, the typical values of material damping of a cantilever beam with circular cross section are 0.02%-0.40% critical damping for SAE 1020 steel (hot rolled), and 0.04%-0.4% for 6063-T6 aluminum. Relative to the other kinds of damping mechanisms, material damping is usually negligible and might be excluded from the analysis.

Fluid damping is a function of support geometry, fluid viscosity, reduced velocity and the density of the fluid. In the case of small amplitude vibrations in a high Reynolds number cross flow, the viscous damping factors for a single mode vibration are given by Blevins [17] as shown in Figure 2.4.

After numerous examples, Blevins [16] advises a critical damping value of 0.9% for the first mode vibration and 0.5% for the third mode vibration of the tubes with clearance supports (loosely held tubes). Pettigrew et al. [24] introduced a reduced damping parameter $c_n = 4 \pi m \mu f/d$ where m is the mass of the tube per unit length, μ is the equivalent critical damping, f and d are the natural frequency and the diameter of the heat exchanger tube respectively. They reported that c_n tends to be constant. For conservative design purposes the reduced damping parameter is taken as 400 for water and 1400 for two-phase flow. The actual damping in the heat exchanger tubes is likely to lie in between these two limiting cases. This formula is not yet reliable due to the insufficient data and the broad range of values. (They reported 8 values for water with a range of $c_n = 372\text{-}672$ kg/(sec.m^2) and 2 values for two-phase mixtures with a range of $c_n = 1407\text{-}3181$ kg/(sec.m^2)).

A realistic mathematical simulation of damping is not possible with the information given in the literature. A damping model is assumed to obtain the effective modes. One

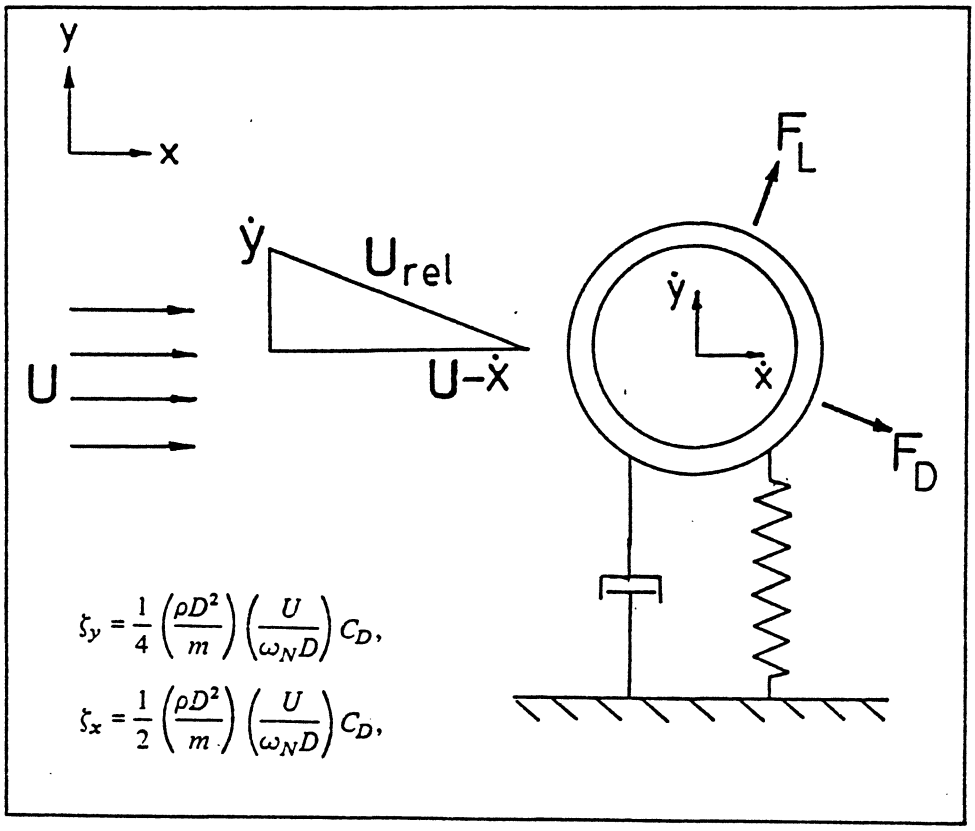

Figure 2.4 Fluid damping.

hypothesized mechanism for the effectiveness of the flat bar support is that the energy is transferred from lower modes to higher modes due to impacting and is dissipated by the higher modes. In order to investigate the modal energy dissipation rates and modal energy contents, a constant modal damping was assumed. Whatever the value of damping, the relative magnitudes of the individual modal dissipation rates would show the contributions of the higher modes to the total energy dissipated. In general it is known that higher modes have lower damping. To be conservative, the constant critical damping value of 1% was assumed for the all modes and the analysis has been carried out using this damping model.

2.2 METHOD OF SOLUTION

The equations of motion for the compete system are given by Equation 2.1. The global stiffness and the global mass matrices in this equation are obtained by rotating (if necessary) and assembling the elemental stiffness and mass matrices. Standard FEM methodology [26] is used to obtain the natural frequencies, mode shapes and the transient response of the heat exchanger tube in the case of no contact. The necessary changes to incorporate the tube-support impacting is discussed in the following sections.

2.2.1 NATURAL FREQUENCIES AND MODE SHAPES

The equations of motion for the free vibration of the complete system can be obtained from Equation 2.1 by letting all the conservative forces be zero. Hence, the damping and the external forces are eliminated and the following equations are obtained:

$$[M]\{\ddot{r}(t)\} + [K]\{r(t)\} = \{0\} \tag{2.2}$$

where [M] and [K] are the reduced global mass and the reduced global stiffness matrices, respectively. Here, the term 'reduced' is used to indicate that the restrained degrees of freedom are eliminated. The sub-space iteration technique is applied to obtain the mode

shapes and eigenvalues of the system. The software developed in the Department of Mechanical Engineering at McMaster University is used for the eigenvalue analysis. In order to calculate the natural frequencies and the mode shapes of the multi-support heat exchanger tubes, these supports are considered as pinned joints, because the baffle thickness/span ratio is rather small. The heat exchanger tube is allowed to rotate freely at the supports due to the support clearance.

2.2.2 NUMERICAL INTEGRATION

The Newmark-β Method, a direct integration technique, is used for integration to obtain dynamic response of the system. The algorithm for this method is given by Bathe and Wilson [25]. This method has usually better accuracy and numerical stability if the integration parameters, α and β, are chosen to be 0.5 and 0.25, respectively.

2.2.3 KINETIC ENERGY, POTENTIAL ENERGY, DISSIPATED ENERGY, AND ENERGY INPUT

Instantaneous values of kinetic and potential energy, dissipated energy, and the energy input to the system is obtained by integrating the equation of motion with respect to displacement. For a single degree of freedom system, the equation of motion is:

$$m\ddot{x}(t) + c\,\dot{x}(t) + k\,x(t) = f(t) \tag{2.3}$$

Integrating Equation 2.5 w.r.t. displacement:

$$\int m\,\ddot{x}(t)\,dx + \int c\,\dot{x}(t)\,dx + \int k\,x(t)\,dx = \int f(t)\,dx \tag{2.4}$$

one can obtain the following :

$\int m\ddot{x}(t)\,dx$: Kinetic energy

$\int c\dot{x}(t)\,dx$: Dissipated energy

$\int k\,x(t)\,dx$: Potential energy

$\int f(t)\,dx$: Energy input

In a more convenient form, kinetic energy can be given as:

$$E_k = \int m\ddot{x}\,dx = m\int \frac{d\dot{x}}{dt}\,dx = m\int \dot{x}\,d\,\dot{x}$$

$$E_k = \frac{1}{2}\,m\,\dot{x}^2 \tag{2.5}$$

Similarly, potential energy is calculated as,

$$E_p = \int kx\,dx = \frac{1}{2}\,k\,x^2 \tag{2.6}$$

These formulae can be modified for finite element application as given below :

Kinetic energy: $$E_k = \frac{1}{2}\{\dot{r}\}^T[M]\{\dot{r}\} \tag{2.7}$$

Potential energy: $$E_p = \frac{1}{2}\{r\}^T[K]\{r\} \tag{2.8}$$

Dissipated energy: $$E_d = \sum \{\dot{r}\}^T[C]\{\Delta r\} \tag{2.9}$$

Energy input: $$E_i = \sum \{F\}^T\{\Delta r\} \tag{2.10}$$

Equations 2.9 and 2.10 can be used to calculate the dissipated energy and the energy input to the system in one integration step simply by removing the summation symbol. One should be careful in calculating the integral (summations for discrete data) given by Equations 2.9 and 2.10, because the velocity and the external force values must be taken at the midpoint of the integration interval (Figure 2.5).

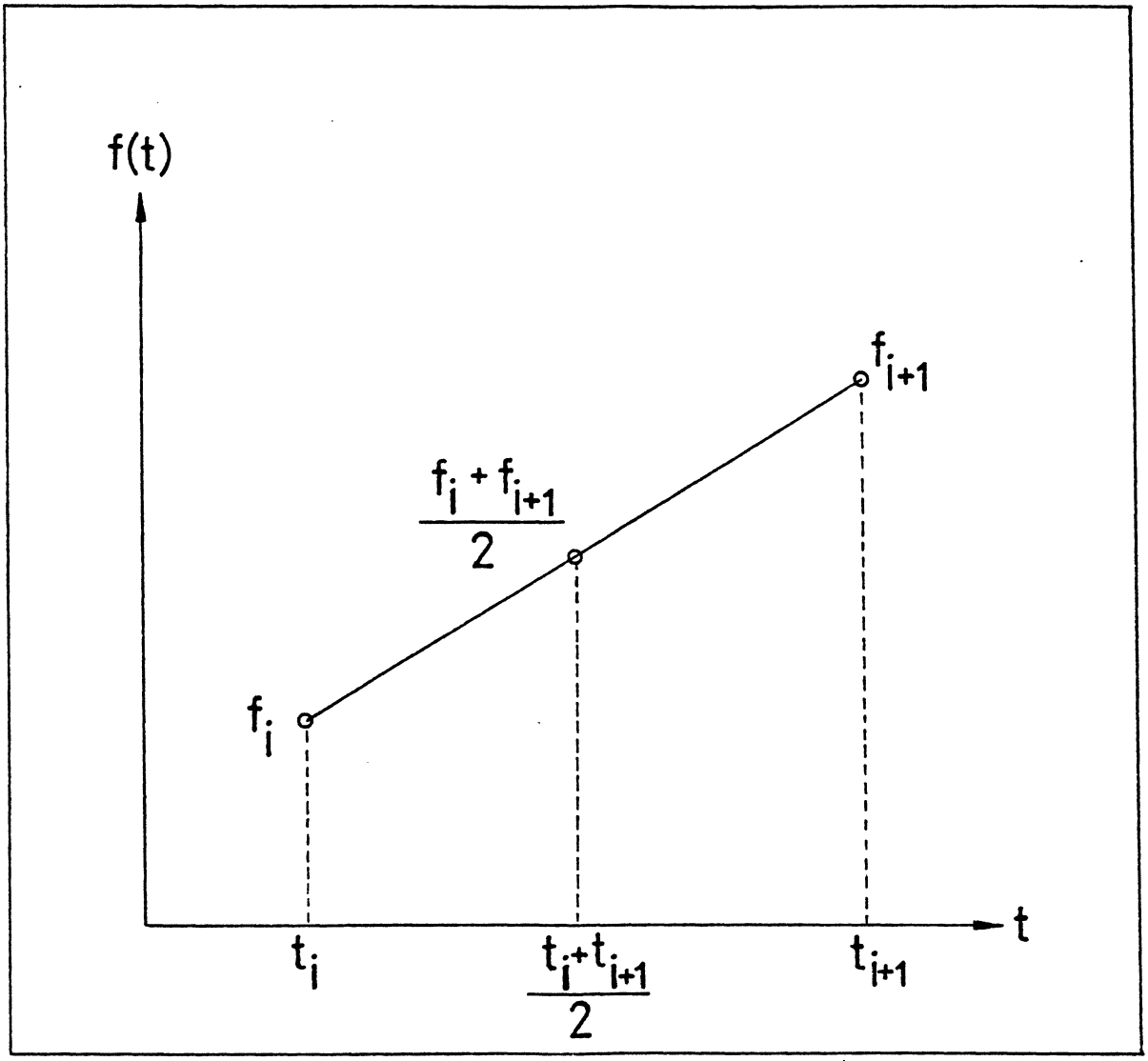

Figure 2.5 Linear interpolation for the midpoints.

The modal kinetic and potential energy values, the energy dissipated by the i'th mode and the energy input to the i'th mode are calculated by :

Kinetic energy:
$$e_{ki} = \frac{1}{2} \dot{q}_i^2 \tag{2.11}$$

Potential energy:
$$e_{pi} = \frac{1}{2} \omega_i^2 q_i^2 \tag{2.12}$$

Dissipated energy:
$$e_{di} = \sum 2 \xi_i \omega_i \dot{q}_i \Delta q_i \tag{2.13}$$

Energy input:
$$e_{ii} = \sum \mathbf{f}_i \Delta q_i \tag{2.14}$$

where q_i are the generalized coordinates. The transformation from cartesian coordinates to the generalized coordinates will be discussed in detail in section 2.2.7 .

2.2.4 EXTERNAL FORCE METHOD

In the case of tube-support impact, the stiffness and damping properties of the system change (see Figures 2.6 and 2.7). Due to hysteretic energy loss, a damping force should be included in Equation 2.1. Due to the support stiffness, an opposing spring force should also be included. The relative motion of the tube with respect to the support on the support surface results in a friction force and therefore a torsional moment on the tube and/or a bending moment depending on the direction of the friction force. These forces and moments must be included in the equations as well. The equations of motion for the external force method are given by Equation 2.15. For the sake of simplicity the time dependence of the vectors are not written.

$$[M]\{\ddot{r}\} + [C]\{\dot{r}\} + [K]\{r\} = \{F_{exc}\}-\{F_{spr}\}-\{F_{dmp}\}-\{F_f\}-\{TQ\} \tag{2.15}$$

where

$\mathbf{F}_{exc}$ is the excitation forcing function

$\mathbf{F}_{spr}$ is the support spring force

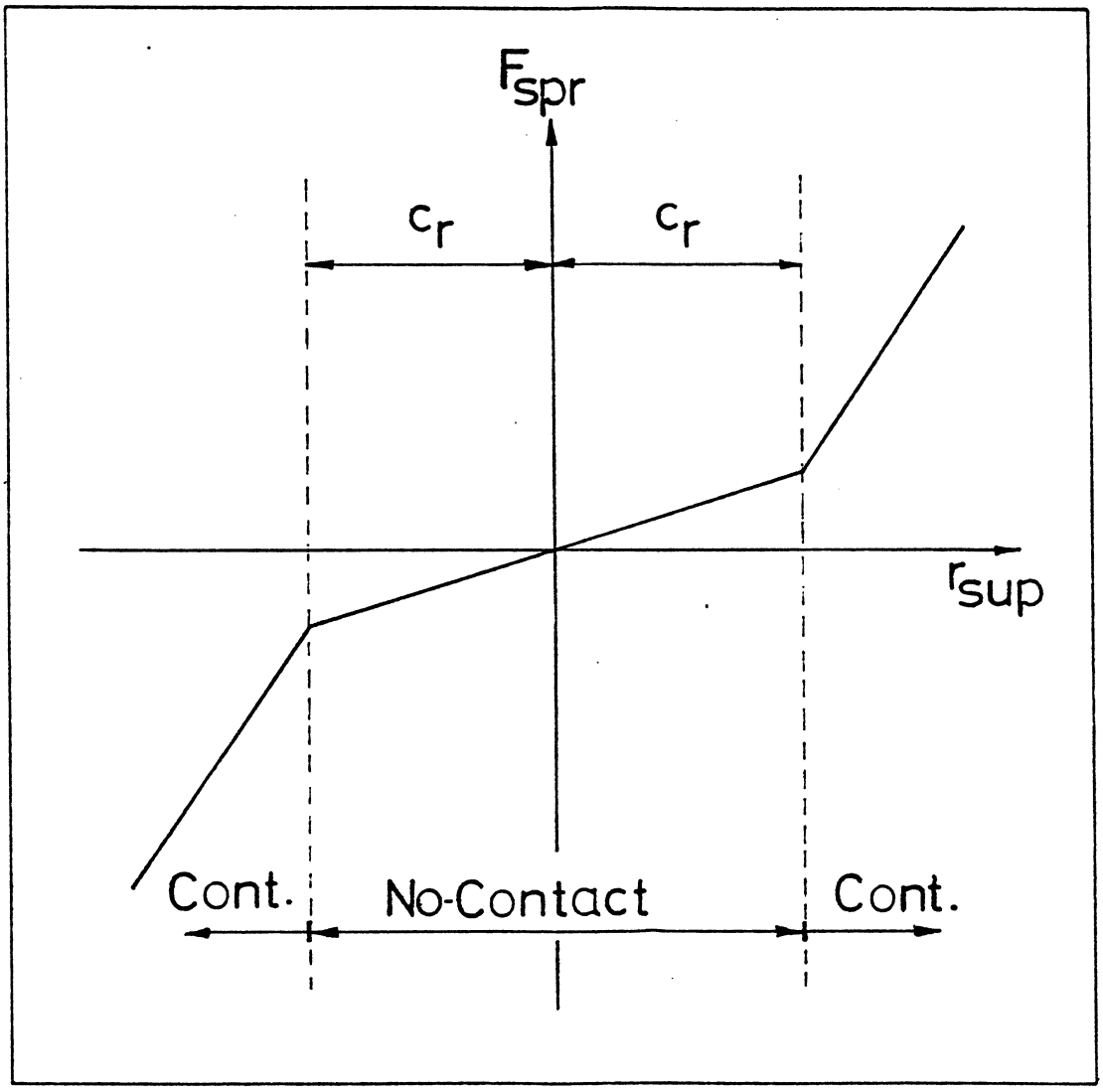

Figure 2.6 Force-displacement relationship in the presence of tube-support clearance.

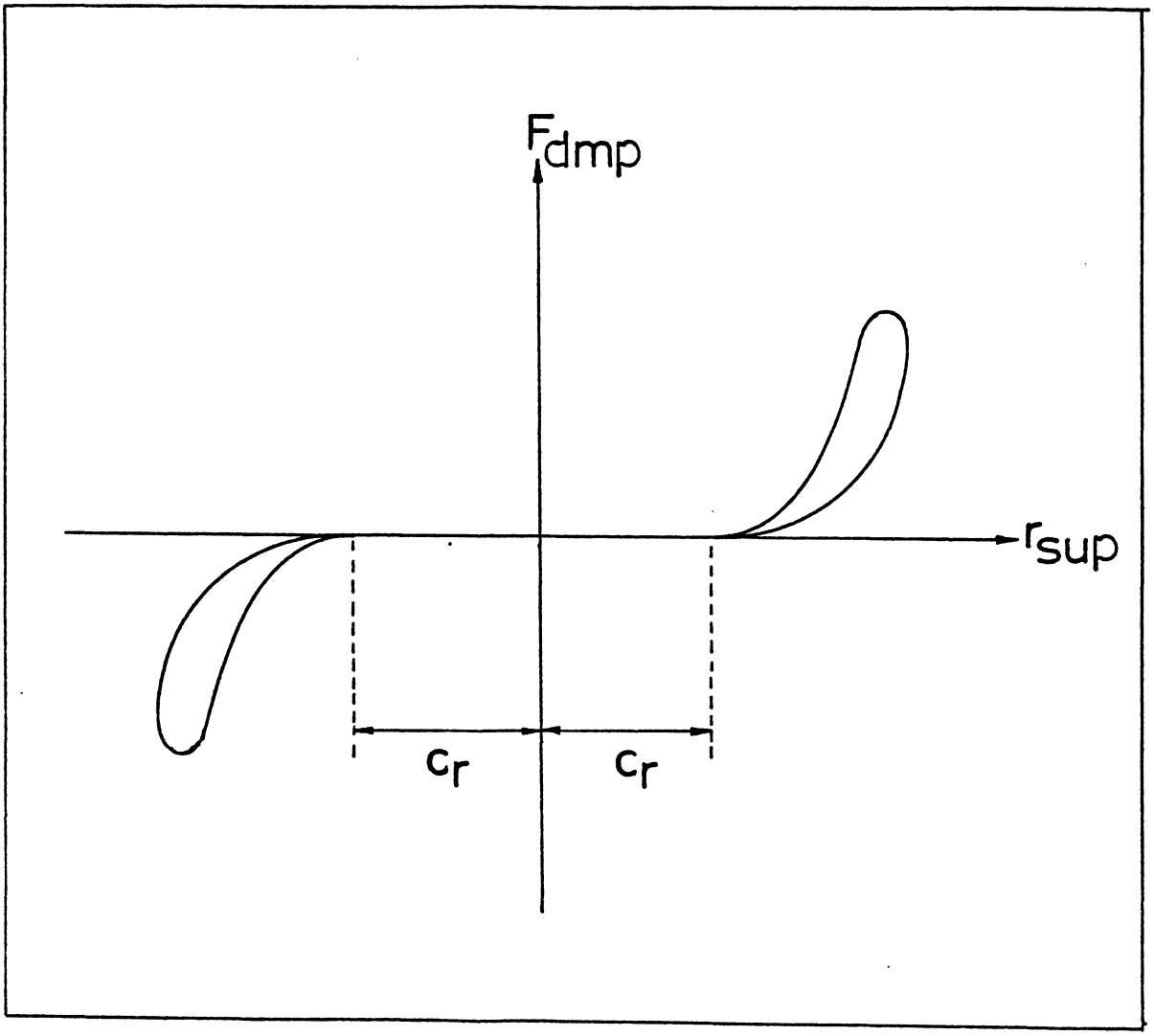

Figure 2.7 Hysterisis loop for contact damping.

$\mathbf{F}_{dmp}$ is the support damping force

TQ is the moment induced by the friction force

If the tube is moving freely (no contact), the spring force, F_{spr}, the damping force, F_{dmp}, and the moment, TQ, are zero. When the displacement of the tube becomes greater than the clearance, contact starts. At this stage, the deflection of the spring, δ_i, and the spring force, F_{spr_i}, are calculated. Since these values are found as if the spring is not opposing the tube motion at i'th integration step, they are overestimated. The spring force at the i'th integration step, F_{spr_i}, is treated as being an external force and other force/moment terms, F_{dmp_i}, F_{f_i} and TQ_i, are calculated by using this value and included as external forces/moments in the same way (Figure 2.8). This method has been used by previous researchers [6]-[12].

2.2.5 THE STIFFNESS METHOD

In this method, the normal impact force is absorbed in the stiffness matrix. That is, the stiffness of the system is changed by adding the support stiffness to the corresponding diagonal terms of the same degrees of freedom. The equations of motion in this case are the following :

$$[M]\{\ddot{r}\} + [C]\{\dot{r}\} + [K_m]\{r\} = \{F_{exc}\}-\{F_{dmp}\}-\{F_f\}-\{TQ\} \tag{2.16}$$

The modified stiffness matrix is given as :

$$[K_m] = [K] + [k_1] + [k_2] + \ldots + [k_{ns}] \tag{2.17}$$

where

[K] is the stiffness matrix in the case of no contact

$[K_m]$ is the modified stiffness matrix in the case of contact

$[k_j]$ is the contribution of the j'th support to the system stiffness matrix

$$m\ddot{r}_{i-1} + c\dot{r}_{i-1} + kr_{i-1} = F_{exc_{i-1}}$$

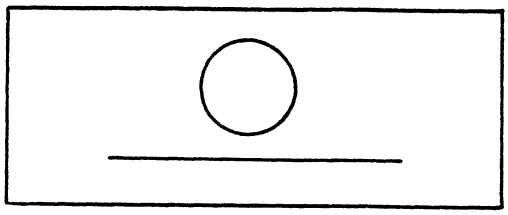

$$m\ddot{r}_i + c\dot{r}_i + kr_i = F_{exc_i}$$

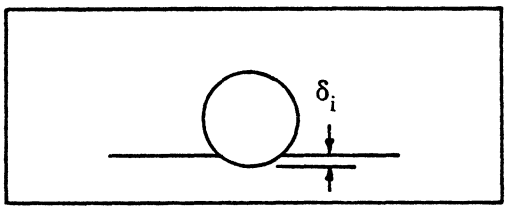

$$m\ddot{r}_{i+1} + c\dot{r}_{i+1} + kr_{i+1} = F_{exc_{i+1}} - F_{dmp_i} - F_{spr_i} - F_{f_i} - TQ_i$$

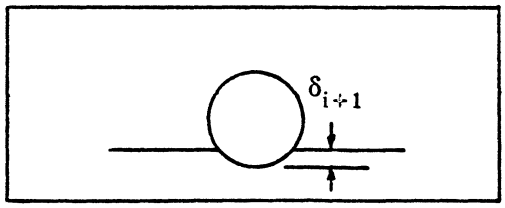

Figure 2.8 The external force method.

$[k_j]$ is the same size as [K] and all the terms except the diagonal ones corresponding to the degrees of freedom in which the j'th support has stiffness contribution, are zeroes.

When the j'th support makes contact with the beam, $[k_j]$ is added to the system stiffness matrix and is subtracted when the contact ceases. In order to save storage area and computation time, only the diagonal elements are stored in the developed FEM program, since the rest of the terms are all zeroes.

In this method, when the tube makes contact with the support, the clearance is modified so that there is no spring deflection (Figure 2.9). The spring stiffness is added to the stiffness of the system to obtain the deflection at $(i+1)$'th integration point, then $F_{spr_{i+1}}$, $F_{dmp_{i+1}}$, $F_{f_{i+1}}$, and TQ_{i+1} are calculated. $F_{dmp_{i+1}}$, $F_{f_{i+1}}$, and TQ_{i+1} are inserted into the force balance of $(i+2)$'th integration step as they are in the external force method.

2.2.6 COMPARISION OF THE EXTERNAL FORCE AND THE STIFFNESS METHOD

These two methods are theoretically the same when the integration time step is infinitely small. Practically, it is not possible to have such time steps and the results might be significantly different from one method to the other if the time steps are not small enough. When the integration time step approaches zero, the results obtained by using these two methods approaches assymptotically to the limiting value. The advantages and disadvantages of these two different methods are tabulated at Table 2.1.

The support stiffness is usually significantly greater than the beam stiffness. This results in very short impact durations relative to the periods of the dominant impact-free modes. Thus, it is necessary to take very much smaller time steps when considering impacting than in the case of no impact. It would be a waste of computation time if the small time step were used over the entire integration period. To reduce computing time, and hence

$$m\ddot{r}_{i-1} + c\dot{r}_{i-1} + kr_{i-1} = F_{exc_{i-1}}$$

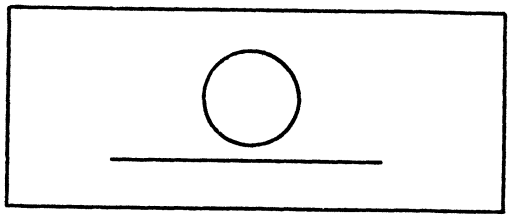

$$m\ddot{r}_{i} + c\dot{r}_{i} + kr_{i} = F_{exc_{i}}$$

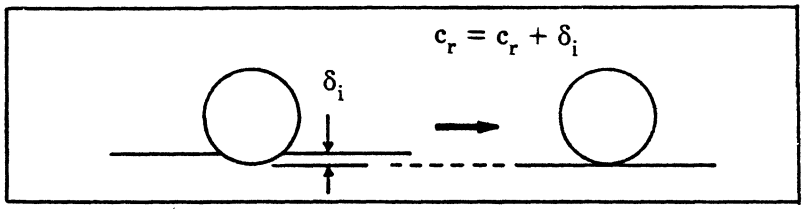

$$m\ddot{r}_{i+1} + c\dot{r}_{i+1} + (k + k_{sp})\, r_{i+1} = F_{exc_{i+1}}$$

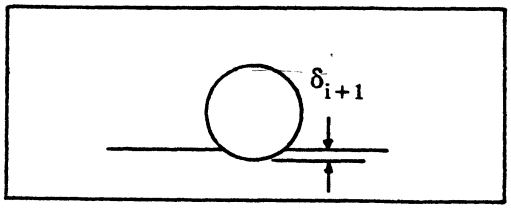

$$m\ddot{r}_{i+2} + c\dot{r}_{i+2} + (k + k_{sp})\, r_{i+2} = F_{exc_{i+2}} - F_{dmp_{i+1}} - F_{f_{i+1}} - TQ_{i+1}$$

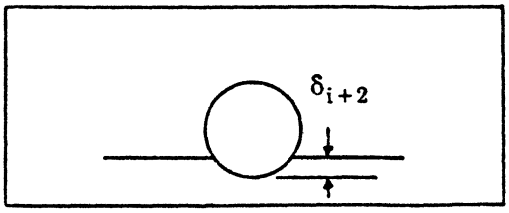

Figure 2.9 The stiffness method.

THE EXTERNAL FORCE METHOD	THE STIFFNESS METHOD
ADVANTAGES	ADVANTAGES
1. Nonlinear spring model can be handled easily.	1. Relatively larger time steps can be used for numerical stability.
2. Easier to program.	2. Impact force calculations are more accurate.
3. Modal analysis is applicable.	
DISADVANTAGES	DISADVANTAGES
1. Not as accurate as the stiffness method.	1. Needs different stiffness matrices for each support combination.
2. Initial spring force is overcalculated which might result in numerical instabilities if the time step is not small enough.	2. Modal analysis is not practical, because the eigenvalues and mode shapes are changing in every contact.
	3. Clearance is modified at each impact to eliminate initial error in spring force.

Table 2.1 Comparison of the external force method and the stiffness method.

the cost, the program was developed to incorporate variation of the time step. In the case of variable time steps, whenever the beam begins contact with the support, the last integration step is repeated with a new and smaller time step. This time step is used until the contact has ended and then another larger time step is used.

The accuracy of these methods lies in the calculation of the initial impact force at the very beginning of the contact. In the external force method, the beam is allowed to penetrate the support at the first integration step of the contact. Therefore, since the deflection of the contact is overestimated at the first time step, the overall impact force is overestimated, although some of the initial error is compensated for during the contact period (Figure 2.8). In the stiffness method, however, when the contact starts, the clearance is modified so that there is no initial penetration. This eliminates the error introduced by the overestimated contact deflection at the begining of the contact. The impact force, on the other hand, is included in the equations of motion, this time internally, by changing the stiffness matrix. Although, the material damping and friction forces and torque and/or bending moment are calculated and still treated as external forces/moments, their effect on the overall displacement response, and hence on the accuracy is not significant.

In general, the external force method requires smaller time increments for numerically stable results. In the trial runs for a cantilever beam with an end support, it was shown that the stiffness method has greater accuracy than the external force method for a given time step. Although, for a single time step the external force method requires 20%-40% less computing time, for the same accuracy the stiffness method requires less computing time. Results for the above mentioned cantilever for a single impact is given in Table 2.2. Convergence of the two methods can also be seen when the time step is decreased, proving that the two methods are equivalent for the limiting case where the time step is very small. Figure 2.10 shows the percent error in impact force values against the number of integration

$l = 1$ [m]

$E = 2.3 \times 10^{11}$ [N/m]

$\nu = 0.3$

$\rho_{sur} = 1.26$ [kg/m^3]

$\rho_b = 1.26$ [kg/m^3]

$k_{sp} = 2.0 \times 10^6$ [N/m]

$d_i = 0.01003$ [m]

$d_o = 0.01588$ [m]

$\alpha = 0.25$ [sec/m]

$\mu = 0.10$

$c_d = 2.5\ 10^{-4}$ [m]

$F(t) = F_{exc}\,\mathrm{Sin}(210.0t)$ at the tip of the cantilever

* Iter./contact	t_c	F_{imp}	% Error
STF. 90	0.0089	15.75	0.00
STF. 36	0.0090	15.77	0.10
STF. 10	0.0090	17.29	9.79
EXT. 90	0.0089	15.91	1.00
EXT. 36	0.0090	16.42	4.25
EXT. 10	0.0090	21.52	36.61

Table 2.2 Comparison of the stiffness method (STF.) and the external force method (EXT.) for the single impact of a cantilever beam.

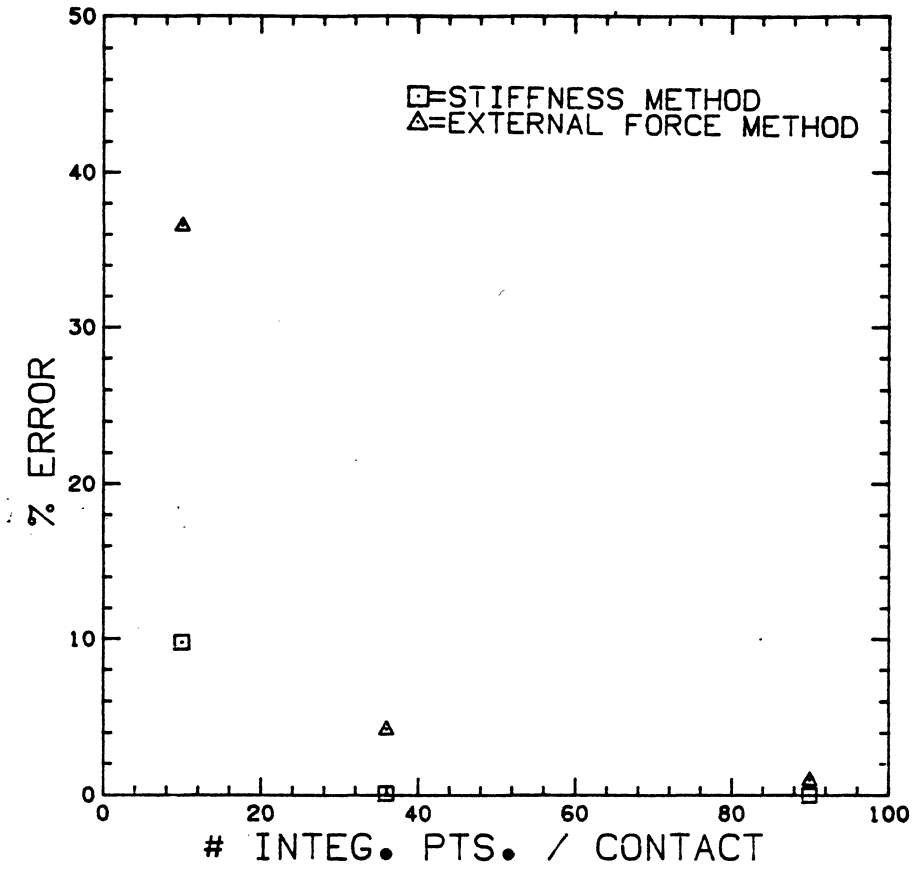

Figure 2.10 Comparison of the external force method and the stiffness method.

points for a single impact. Percent error values are calculated by taking the 90 iteration/contact stiffness method solution as a reference point. For reasonable accuracy and numerical stability, the author advises at least 10 integration steps during a beam-support contact for the stiffness method and 20 integration steps for the external force method. The error in the calculated impact force is not cumulative. Therefore, a numerically stable solution does not necessarily ensure accurate results. In the case where there is a very short contact duration where the time step is chosen for the characteristic longer contacts, an apparently stable solution may suddenly become unstable. In the case of numerical instability, error is cumulative. Once the instability starts, a numerical overflow occurs within a few steps and the program is aborted. Since the contact duration is determined by the stiffness of the support, excitation forcing function and clearance, the time step might need to be changed if these parameters are changed in different runs. It is advised for numerically stable results with reasonable accuracy that the time step to be taken should be about one tenth of the period of the highest mode included in the analysis. In the external force method, calculated impact force levels might be up to 40%-50% higher than the values found by using very small time step, although there is no numerical instability observed. In the stiffness method, numerically stable results usually ensure an upper error limit of about 15%-20%.

In the case of multi-support beams, the cost of the computation using stiffness method increases, because the system stiffness matrix is changed every time when the impact starts and ends. Stiffness values are read from the tapes and added (or subtracted) to (from) the main system stiffness matrix. The number of impacts is the determining factor of the cost. The greater the number of contacts, the longer the computer run. This is, again, a function of system parameters, namely, clearance,support stiffness, and the excitation forcing function. Once the system parameters are fixed, it is easily found which method would be cheaper by

means of a few test runs. In general, the stiffness method is more advantageous than the external force method if there are only a few supports. Most researchers have not used more than a few supports for this kind of impact problem due to the difficulties in interpreting the results (both experimental and computational). The reason is that the non-linearity does not allow the use of superposition.

One main advantage of the external force method over the stiffness method is that it allows the use of modal analysis which reduces the computing cost by minimizing the half bandwidth of the global matrices. In this case, the user can afford smaller time steps for greater accuracy. Modal analysis also enables one to eliminate the unwanted modes from the analysis. These are powerful tools in vibration analysis. However, the reason that the modal analysis was used in this research is because it was an intention of this study to model a constant modal damping in order to investigate the relative importance of the modes.

2.2.7 MODAL ANALYSIS

Modal analysis is necessary in order to input constant modal damping values. This also facilitates the calculation of modal energies and modal cumulative energy losses. Additionally, modal analysis has the potential to decrease the computation cost as stated above. Modal analysis cannot be incorporated with the stiffness method, because the eigenvalues and the eigenvectors of the system change every time the tube contacts one of the supports. If there are N_S supports, then $N_S!$ sets of eigenvalues and eigenvectors are needed to carry out the analysis in the stiffness method. Therefore, between the two methods investigated, the external force method was chosen to incorporate the modal analysis.

Once the eigenvalues and the mode shapes of the system are obtained as discussed in section 2.2.1, equations of motion can be decoupled by means of the following coordinate transformation :

$$\{r(t)\} = [\Phi]\{q(t)\} \tag{2.18}$$

where

$[\Phi]$ is $[\phi_1, \phi_2, ..., \phi_n]$, is the transformation matrix

$\{\phi_i\}$ is the i'th mode shape

$\{q(t)\}$ is the displacement array in generalized coordinates

For simplicity, $[\Phi]$ is M-orthonormalized; i.e.,

$$\{\phi_i\}^T [M] \{\phi_j\} = \delta_{ij} \tag{2.19}$$

where δ_{ij} is the Kronecker delta. This makes the transformed mass matrix the unit diagonal matrix. The transformed stiffness matrix is also a diagonal matrix, the diagonal terms being the eigenvalues as given below :

$$[\Phi]^T [K] [\Phi] = \begin{bmatrix} \omega_1^2 & & & & \\ & \omega_1^2 & & & \\ & & \cdot & & \\ & & & \cdot & \\ & & & & \omega_n^2 \end{bmatrix} = \begin{bmatrix} \omega_i^2 \end{bmatrix} \tag{2.20}$$

Substituting Equation 2.16 in Equation 2.1 and premultiplying the equation by $[\Phi]^T$ the following is obtained :

$$\{\ddot{q}\} + [\Phi]^T [C] [\Phi] \{\dot{q}\} + \begin{bmatrix} \omega^2 \end{bmatrix} \{q\} = [\Phi]^T \{F\} \tag{2.21}$$

The transformed damping matrix is not necessarily a diagonal matrix. If the damping matrix is chosen to be a linear function of the mass and the stiffness matrices, Equation 2.1 gives a set of uncoupled equations of motion. In this case the damping can be found by,

$$[C] = c_1[M] + c_2[K] \tag{2.22}$$

where c_1 and c_2 are two constants to be determined according to the damping values. If the modal damping values are known or can be estimated, they can be directly input by taking, $c_{ij} = 2\ \omega\ \xi_i \delta_{ij}$, where ξ_i is the critical modal damping. In direct integration algorithms, like the Newmark-β method, the number of operations required is directly proportional to the half

bandwidth of the stiffness matrix. By decoupling the equations of motion, the half bandwidth of the stiffness matrix decreases. When it is necessary to carry out the integration process many times, the decoupling of the equations of motion might significantly decrease computing cost. It is also possible to eliminate the unwanted modes to save computing time, once the modes are uncoupled.

2.2.8 MODE COUPLING OF HEAT EXCHANGER U-TUBES

A schematic drawing of a heat exchanger U-tube assembly is given in Figure 2.11. In this structure, in-plane and out-of-plane modes are uncoupled if there is no intermittent support. The motion in the x-y plane is defined as being in-plane motion and the motion perpendicular to this plane is defined as being the out-of-plane motion. The uncoupled in-plane and out-of-plane modes are associated with the degrees of freedom (x,y,θ_z) and (z,θ_x,θ_y), respectively. Equation 2.18 gives the following uncoupled modal equations of motion for in-plane and out-of-plane modes for the no contact case :

$$\text{In-plane} \qquad \ddot{q}_i + 2\,\xi_i\,\omega_i\,\dot{q}_i + \omega_i^2\,q_i = \{\phi_i\}^T\{F\} = f_i d \tag{2.23}$$

$$\text{Out-of-plane} \qquad \ddot{q}_o + 2\,\xi_o\,\omega_o\,\dot{q}_o + \omega_o^2\,q_o = \{\phi_o\}^T\{F\} = f_o d \tag{2.24}$$

where, $\{\phi_o\}$ is an out-of-plane mode shape. The values corresponding to the in-plane degrees of freedom, namely, x,y, and θ_z are then zero in out-of-plane mode shapes. Hence, f_o has no contribution from the in-plane forcing functions. Similarly, f_i has no contribution from the out-of-plane forcing functions. Therefore, in-plane and out-of-plane modes are independent.

If a flat-bar support is introduced at the apex, an impact force is included in {F} which is a function of the out-of-plane displacements. When there is motion of the tube along the support surface, the normal impact force will produce a friction force in the in-plane directions. This force eventually changes the in-plane displacements, coupling the in-plane modes with the out-of-plane modes. The friction force on the support surface can be expressed

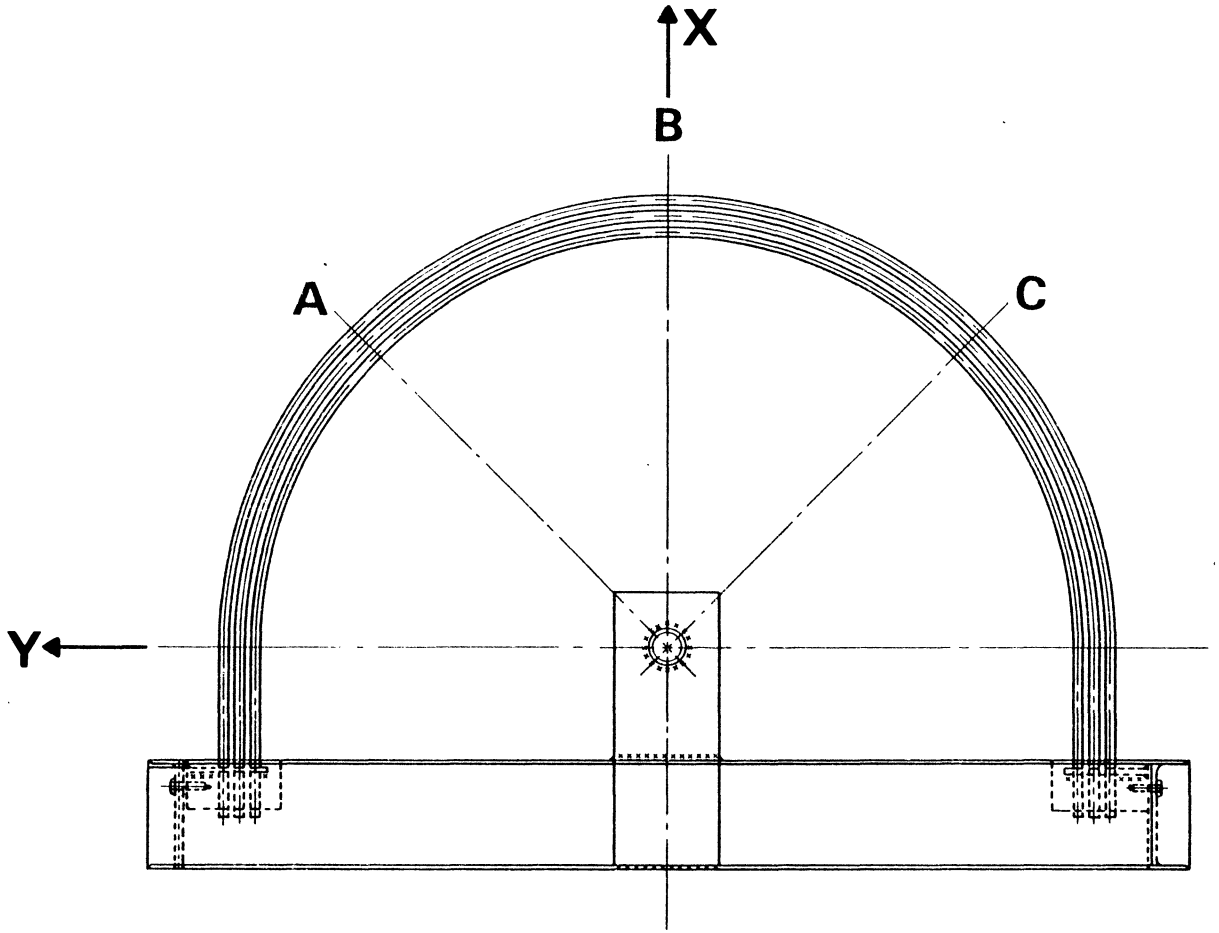

Figure 2.11 Heat exchanger U-tube assembly (adapted from [2]).

with two components along the x and y axes. The one along the x axis creates a local torque (torque at point A, bending moment at points B and C) which alters the out-of-plane motion as well. When out-of-plane motion changes, in-plane motion changes due to the varying impact force (i.e. the friction force) and so forth. The equations of motion for the "contact" case takes the following form :

In-plane

$$\ddot{q}_i + 2\,\xi_i\,\omega_i\,\dot{q}_i + \omega_i^2\,q_i = f_i - f_f - TQ_i \,. \tag{2.25}$$

Out-of-plane

$$\ddot{q}_o + 2\,\xi_o\,\omega_o\,\dot{q}_o + \omega_o^2\,q_o = f_o - f_{spr} - f_{dmp} - TQ_o \tag{2.26}$$

For the special case investigated in this study where the flat bar supports are in the plane of U-bend, the moment terms are associated only with the out-of-plane degrees of freedom and the TQ_i term drops from Equation 2.25.

CHAPTER 3

MATHEMATICAL MODELLING OF TUBE-SUPPORT INTERACTION

In order to accommodate tube enlargement and motion caused by thermal expansion, and because of unavoidable manufacturing tolerances, there is usually clearance between heat exchanger tubes and supports. This makes the tube-support interaction highly nonlinear, since the stiffness and damping properties of the structure change sharply when the tube contacts a support.

In this section, modelling of the flat bar supports used in this analysis is discussed. Impact force, friction force, and torque are also formulated to investigate friction damping and energy transfer by means of mode coupling.

3.1 A MODEL FOR FLAT BAR SUPPORTS

In heat exchangers, flat bars support more than one tube at the same time (Figure 3.1). To investigate the dynamic behaviour of a single tube, the structure to be analysed can be reduced to a single tube and two flat bar supports, one at each side, with moving boundaries (Figure 3.2). The exact nature of the motion of a flat bar support is influenced by the continuous impacting of all the tubes which it supports. Since it is not a practical approach to include all of the heat exchanger tubes in the analysis, the idea of determining the boundary motions was eliminated. Instead, the flat bar supports are modelled as a fixed spring-damper system due to the significantly lower displacements of the supports relative to the displacements of the heat exchanger tubes. As a result, the system under consideration takes the final form shown in Figure 3.3. This model neglects fluid and mechanical coupling of the tubes. Since the equivalent concentrated mass of the tube at the support is an order of

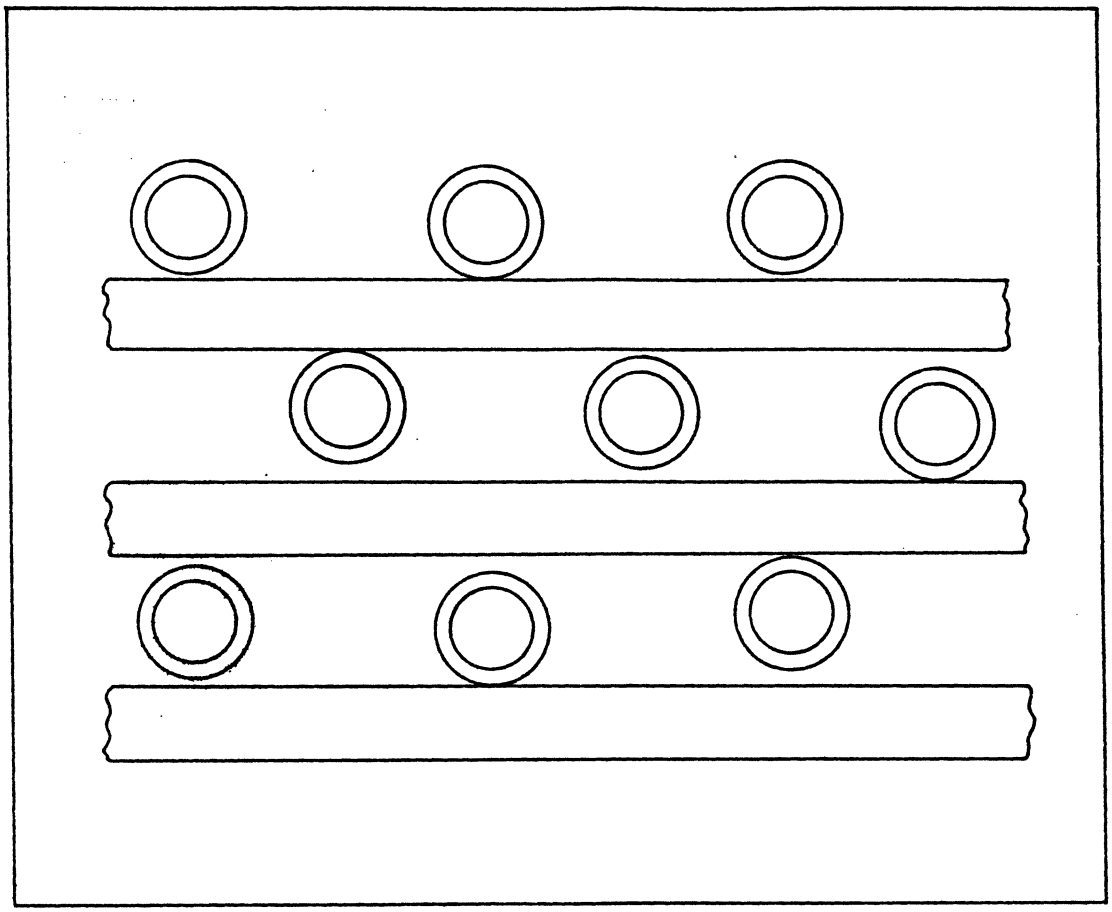

Figure 3.1 Heat exchanger tubes with flat bar supports.

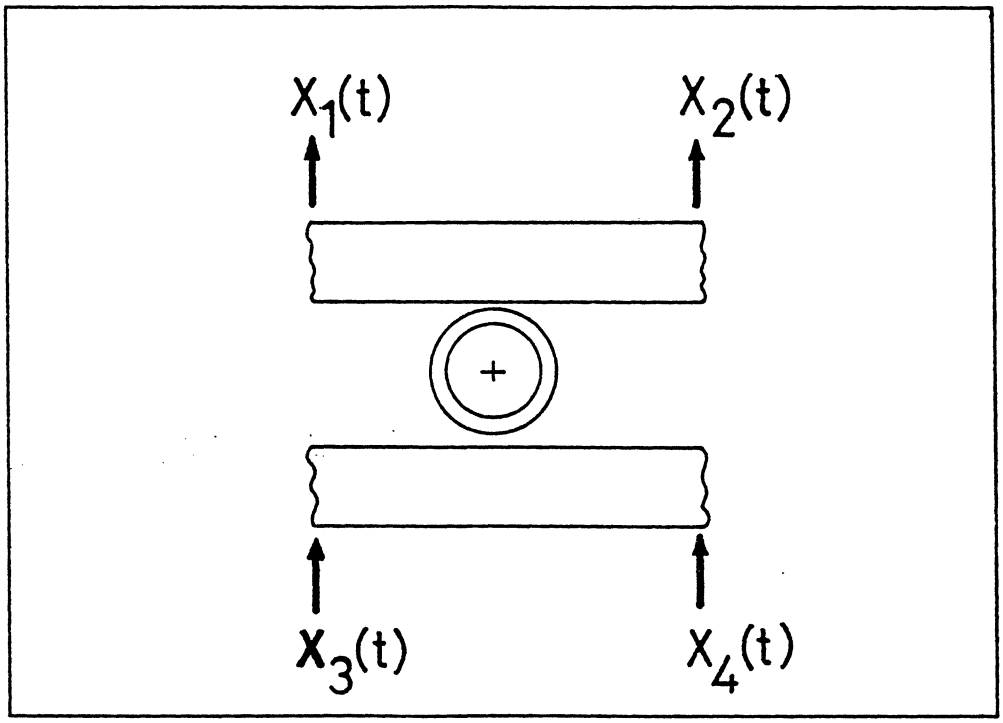

Figure 3.2 Simplified model for flat bar supports with moving boundaries.

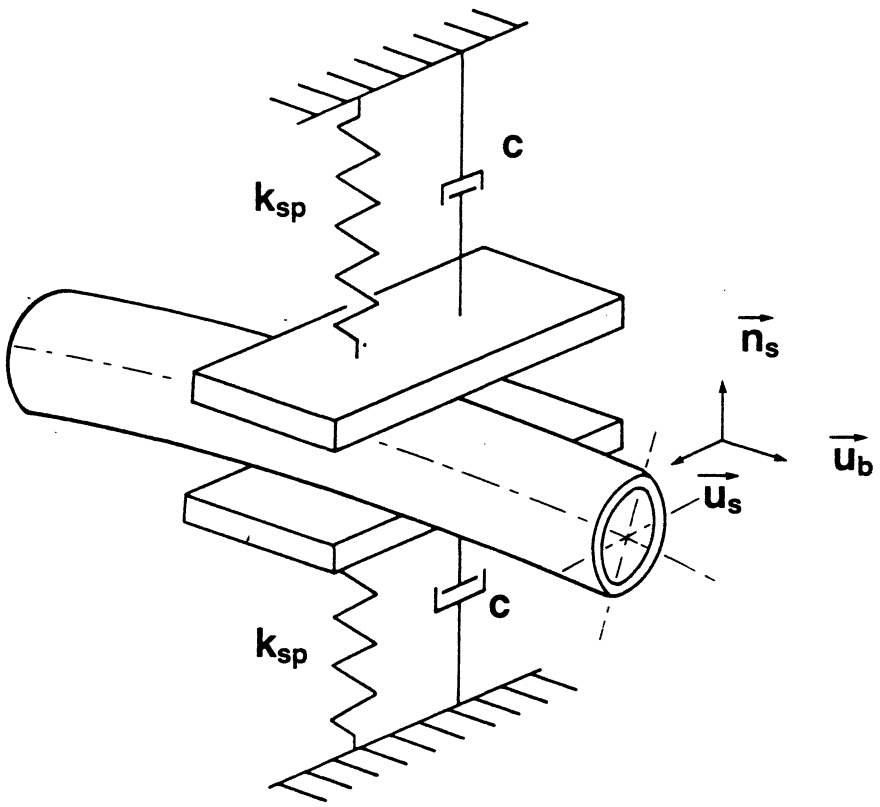

Figure 3.3 Spring-damper model for the flat bar supports.

magnitude higher than the mass of the flat bars, the flat bar masses are neglected. The support stiffness, k_{sp}, is a function of tube support geometry and the material properties. An experimental range of 10^6-10^7 N/m has been reported by previous researchers [8]-[9] and is considered to be valid for the geometry under consideration. Rogers and Pick [8] reported a change of only a few percent in RMS impact forces when the stiffness was increased four times. Therefore a stiffness value in the above mentioned range should give reasonable and consistent results, even if the stiffness is substantially in error. A stiffness value of 2.0×10^6 N/m is used throughout this study. The support material damping force is calculated by using the following relationship [23]:

$$F_{dmp} = 1.5\,\alpha\, k_{sp}\,\delta\,\dot{\delta} = 1.5\,\alpha\,\dot{\delta}\,F_{imp} \tag{3.1}$$

where δ is the support deflection and the dot refers to differentiation with respect to time. The value of the material damping constant, α, is 0.25 sec/m for steel [23].

3.2 THE SPRING FORCE

The position vector of the tube's centre is,

$$\mathbf{r} = r_x\,\mathbf{i} + r_y\,\mathbf{j} + r_z\,\mathbf{k} \tag{3.2}$$

where, r_x, r_y, and r_z are the displacements and **i**, **j**, and **k** are the unit vectors along x,y, and z axes, respectively. Velocity, **v**, and acceleration, **a**, are found by differentiating Equation 3.6.

$$\mathbf{v} = \frac{d\mathbf{r}}{dt} = \dot{r}_x\,\mathbf{i} + \dot{r}_y\,\mathbf{j} + \dot{r}_z\,\mathbf{k} \tag{3.3}$$

$$\mathbf{a} = \frac{d^2\mathbf{r}}{d^2t} = \ddot{r}_x\,\mathbf{i} + \ddot{r}_y\,\mathbf{j} + \ddot{r}_z\,\mathbf{k} \tag{3.4}$$

The unit normal vector of the support surface is given by,

$$\mathbf{n_s} = (n_{xs}\,\mathbf{i} + n_{ys}\,\mathbf{j} + n_{zs}\,\mathbf{k}) \tag{3.5}$$

where

$n_{xs} = \mathrm{Cos}\theta_x$, θ_x is the angle between $\mathbf{n_s}$ and the x axis

$n_{ys} = \text{Cos}\theta_y$, θ_y is the angle between $\mathbf{n_s}$ and the y axis

$n_{zs} = \text{Cos}\theta_z$, θ_z is the angle between $\mathbf{n_s}$ and the z axis

The unit vector along the beam is calculated by using the nodal coordinates as follows,

$$\mathbf{u_b} = [(x_{i+1} - x_i)\mathbf{i} + (y_{i+1} - y_i)\mathbf{j} + (z_{i+1} - z_i)\mathbf{k}] / l_e \tag{3.6}$$

and

$$l_e = [(x_{i+1} - x_i)^2 + (y_{i+1} - y_i)^2 + (z_{i+1} - z_i)^2]^{1/2} \tag{3.7}$$

Two vectors are required to define the support plane $\mathbf{n_s}$. Therefore, to define the support plane, the unit vector $\mathbf{u_b}$ is used along with the unit vector $\mathbf{u_s}$, which is obtained by taking the cross product of $\mathbf{u_b}$ and $\mathbf{n_s}$ (See Figure 3.4).

$$\mathbf{u_s} = \mathbf{u_b} \times \mathbf{n_s} \tag{3.8}$$

The total displacement toward the support, r_{sup}, is found by,

$$r_{sup} = \mathbf{r}.\mathbf{n_s} = r_x n_{xs} + r_y n_{ys} + r_z n_{zs} \tag{3.9}$$

Since there are two flat bar surfaces, one on each side of the tube, and a single unit normal vector, $\mathbf{n_s}$, the sign of r_{sup} will be dependent on which support the tube is moving towards. To eliminate the sign confusion which causes problems in the force calculations, the unit normal vector, $\mathbf{n_s}$, is modified such that it always points outwards from the support surfaces as seen in Figure 3.5. The modified unit normal vector, $\mathbf{n_{sm}}$, is,

$$\mathbf{n_{sm}} = -\text{Sign}(\mathbf{r}.\mathbf{n_s})\,\mathbf{n_s} = -\text{Sign}(r_{sup})\mathbf{n_s} \tag{3.10}$$

When r_{sup} is equal to or greater than the radial clearance, c_r, the tube and support are in contact and the contact deflection is found as,

$$\delta = |r_{sup}| - c_r \tag{3.11}$$

where c_r is half of the diametral clearance c_d. The spring force is then calculated by,

$$F_{spr} = k_{sp}\,\delta \tag{3.12}$$

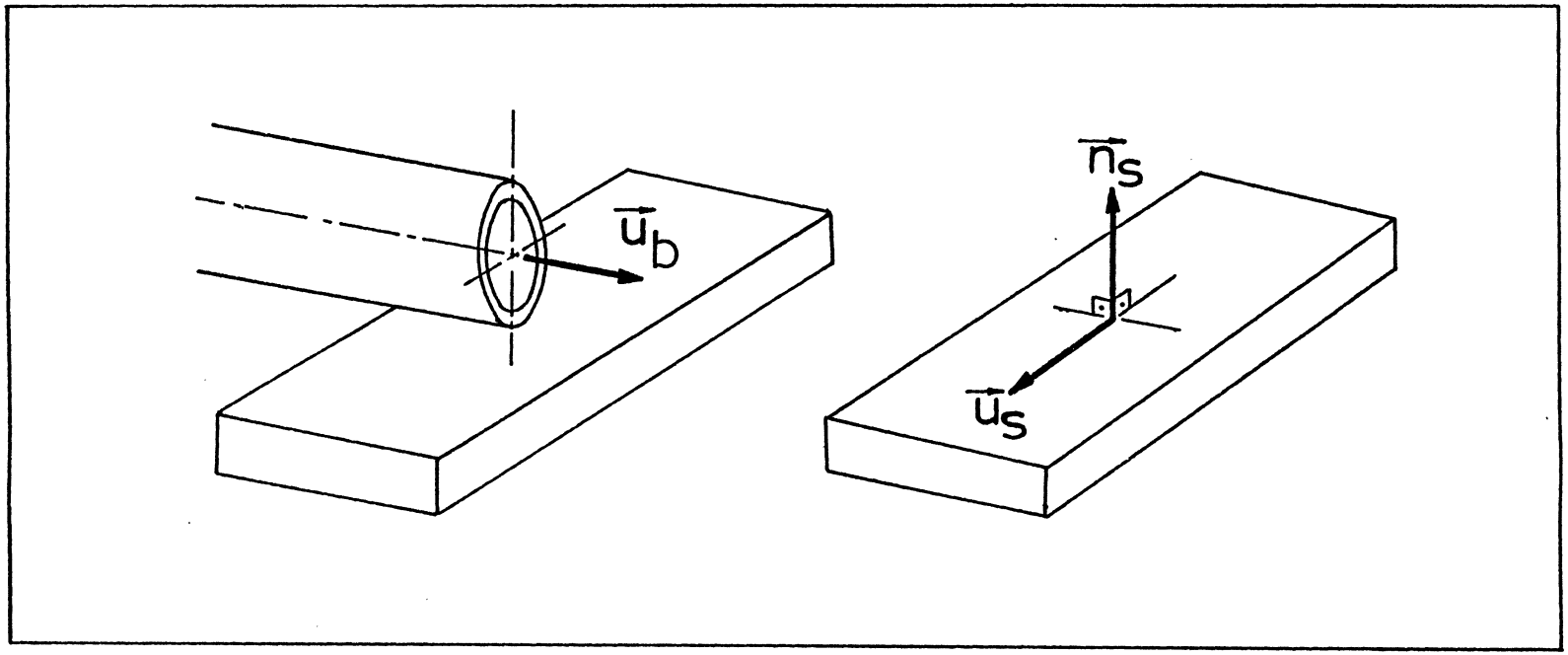

Figure 3.4 Flat bar support tube geometry.

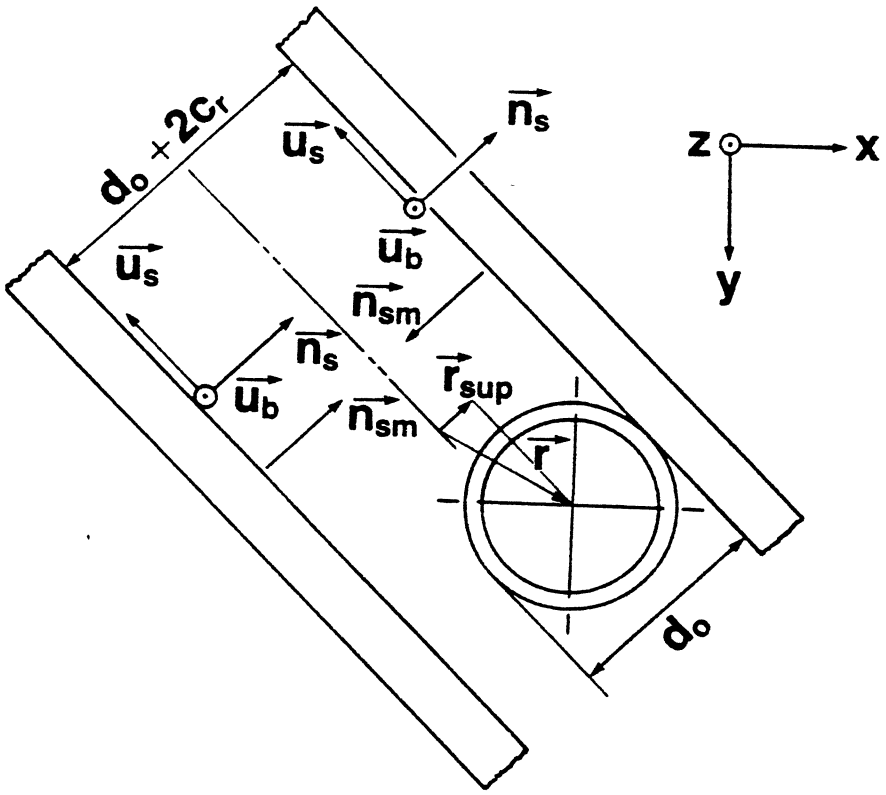

Figure 3.5 Schematic drawing of the mathematical model.

The spring force acting on the tube always points out of the support surfaces as the modified unit normal vector does. In order to find the components of the spring force in the x,y, and z directions, the magnitude of the spring is multiplied by the modified unit normal vector given by Equation 3.10,

$$\mathbf{F_{spr}} = F_{spr}\,\mathbf{n_{sm}} \tag{3.13}$$

3.3 SUPPORT DAMPING FORCE

The support damping force given by Equation 3.1 is rewritten for this case as shown in Equation 3.14,

$$F_{dmp} = 1.5\,\alpha\,F_{spr}\,|\mathbf{n_{sm}}.\mathbf{v}| \tag{3.14}$$

The damping force is along $\mathbf{n_{sm}}$ when the tube is moving into the support (velocity component along $\mathbf{n_{sm}}$ is negative), and it is along $-\mathbf{n_{sm}}$ when the tube is moving out of the support (velocity component along $\mathbf{n_{sm}}$ is positive). Therefore, Equation 3.14 is modified for vectorial notation as given below :

$$\mathbf{F_{dmp}} = -\text{Sign}(\mathbf{n_{sm}}.\mathbf{v})\,1.5\,\alpha\,F_{dmp}\,\mathbf{n_{sm}} \tag{3.15}$$

3.4 FRICTION FORCE

If there is relative motion between the tube and the support on the support surface, a friction force is induced. This force always opposes the motion and acts like a damping mechanism. Coulomb's model of friction assumes a linear relationship between the friction force and the normal force as follows :

$$F_f = \mu\,F_{imp} \tag{3.16}$$

where

μ is the coefficient of friction,

$\mathbf{F_{imp}} = \mathbf{F_{spr}} + \mathbf{F_{dmp}}$ is the impact force

The friction force has components along $\mathbf{u_s}$ and $\mathbf{u_b}$, the two unit vectors defining the support surface. Velocity components along $\mathbf{u_s}$ and $\mathbf{u_b}$ are found by :

$$v_{us} = \mathbf{u_s}.\mathbf{v} \tag{3.17}$$

$$v_{ub} = \mathbf{u_b}.\mathbf{v} \tag{3.18}$$

Since the friction force is opposing the motion, it is rewritten in vectorial notation as shown in Equation 3.19 .

$$\mathbf{F_f} = \mathbf{F_{fus}} + \mathbf{F_{fub}} \tag{3.19}$$

where

$\mathbf{F_{fus}} = -\text{Sign}(\mathbf{u_s}.\mathbf{v})\, F_f\, \mathbf{u_s}$ is the friction force along $\mathbf{u_s}$

$\mathbf{F_{fub}} = -\text{Sign}(\mathbf{u_b}.\mathbf{v})\, F_f\, \mathbf{u_b}$ is the friction force along $\mathbf{u_b}$

The friction force acts tangentially on the circumference of the tube. This force is to be translated to the centre of the tube. $\mathbf{F_{fus}}$ creates an equivalent local torque-force pair. This local torque acts in some cases like a bending moment when the global system is considered. For example, this happens in U-tubes with a support at the apex. Similarly, $\mathbf{F_{fub}}$ creates an equivalent local bending moment-force pair at the centre of the tube. This pair has global torsional effects in U-tubes. The moments (bending moment and torsion) created by the friction force is determined by,

$$TQ = R\, F_f \tag{3.20}$$

where R is the outer radius of the tube. Vectorially, R should be taken in the opposite direction of $\mathbf{n_{sm}}$ for the torque calculation. This gives the following equation for the moments,

$$\mathbf{TQ} = \mathbf{R} \times \mathbf{F_f} = -(R\, \mathbf{n_{sm}}) \times \mathbf{F_f} \tag{3.21}$$

CHAPTER 4

RESULTS AND DISCUSSION

A beam finite element program was developed to investigate the dynamic response of the heat exchanger U-bend tubes in three dimensional space. This program was modified to investigate tube-support impacting due to support clearance. Two methods were used to the above mentioned program. The first approach is the traditional external force method which has been used previously by the other researchers [6]-[9]. The other one is the stiffness method which is introduced in this study. It was shown in Chapter 2 that these two methods are equivalent when the time step approaches zero. Their relative advantages and disadvantages are also discussed in the same chapter. Both of these programs were further modified to incorporate the change in time step because the requirement of using a very small time step due to impacting is a waste of computing time during the period in which there is no contact. Percent (and/or absolute) modal kinetic and potential energies, energy input per time step, total energy input, modal energy losses per time step and modal cumulative energy losses were also calculated. The energy balance is checked every 50 integration time steps.

4.1 SYSTEM PARAMETERS

As an example, a cantilever beam with an end support is taken into consideration (Table 4.1). It was excited with the same sinusoidal force in the in-plane and out-of-plane directions. 1% critical damping was applied to each mode.32 modes were used in analysis. Percent modal energies and percent cumulative energy losses are given in Figures (4.3-4.4). Figures (4.1-4.2) are the displacement-time and the impact force-time plots, respectively. As it is seen, energy contents and energy losses of the higher modes increase when tube-support

L	= 1	[m]
E	= $2.3\ 10^{11}$	[N/m]
ν	= 0.3	
ρ_{sur}	= 1.26	[kg/m^3]
ρ_b kl	= 7920.0	[kg/m^3]
k_{sp}	= 2.0×10^6	[N/m]
d_i	= 0.01003	[m]
d_o	= 0.01588	[m]
α	= 0.25	[sec/m]
μ	= 0.10	
c_d	= 2.5×10^{-4}	[m]
F(t)	= F_{exc}Sin (210.0t) at the tip of the cantilever	

Table 4.1 The system parameters of the cantilever beam

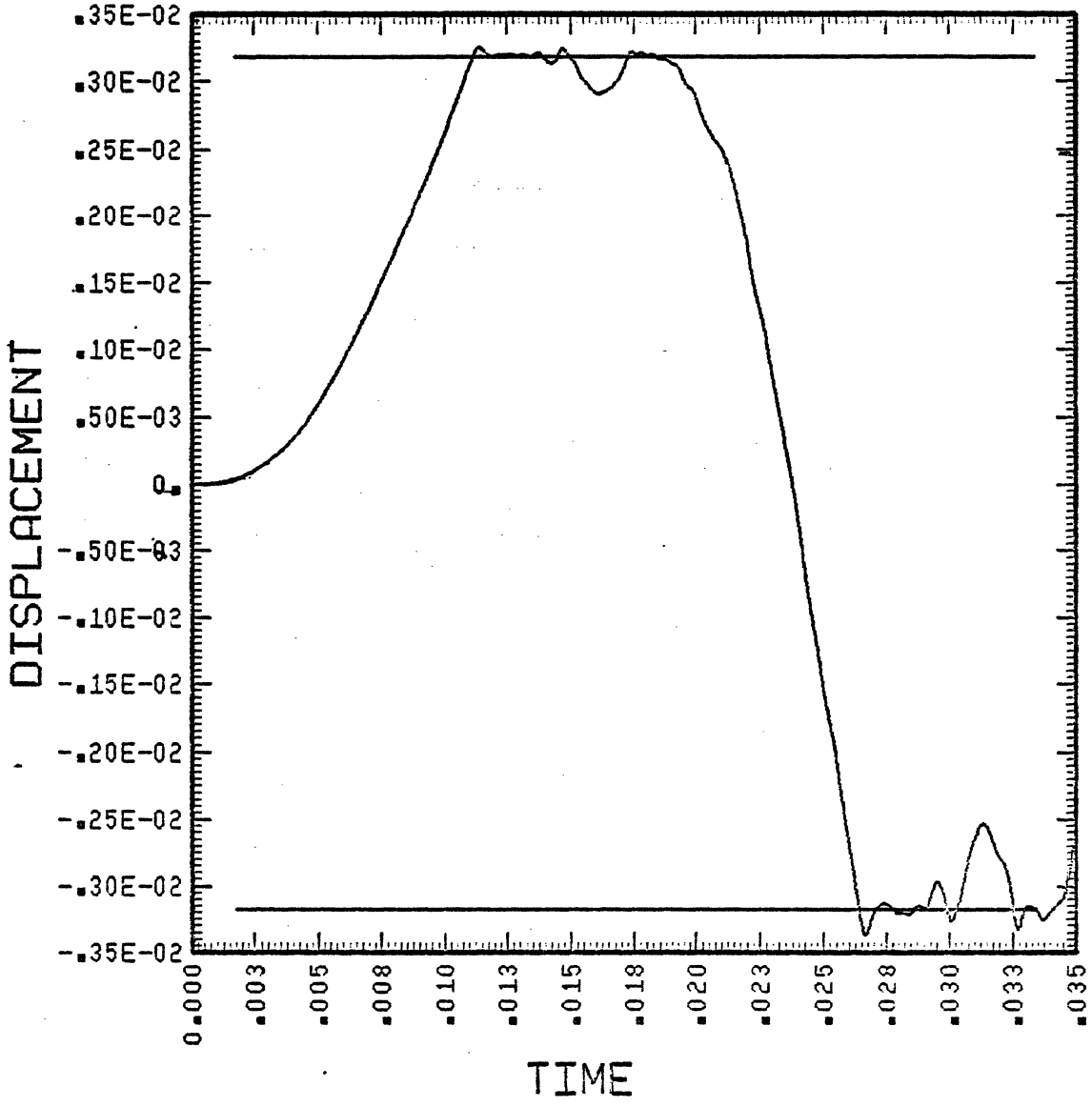

Figure 4.1 Displacement history of the cantilever beam with flat bar supports.

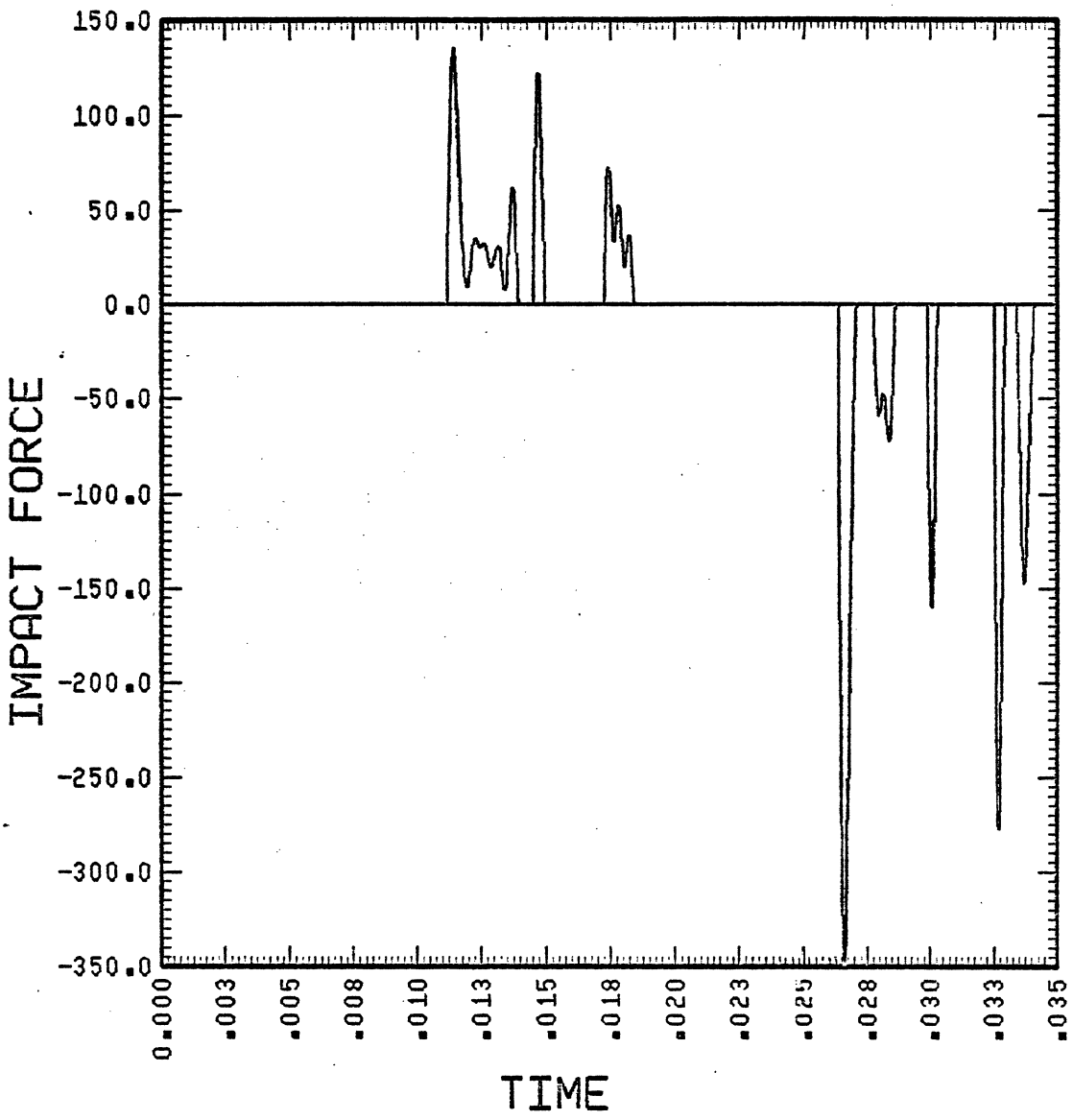

Figure 4.2 Impact force history of the cantilever beam with flat bar supports.

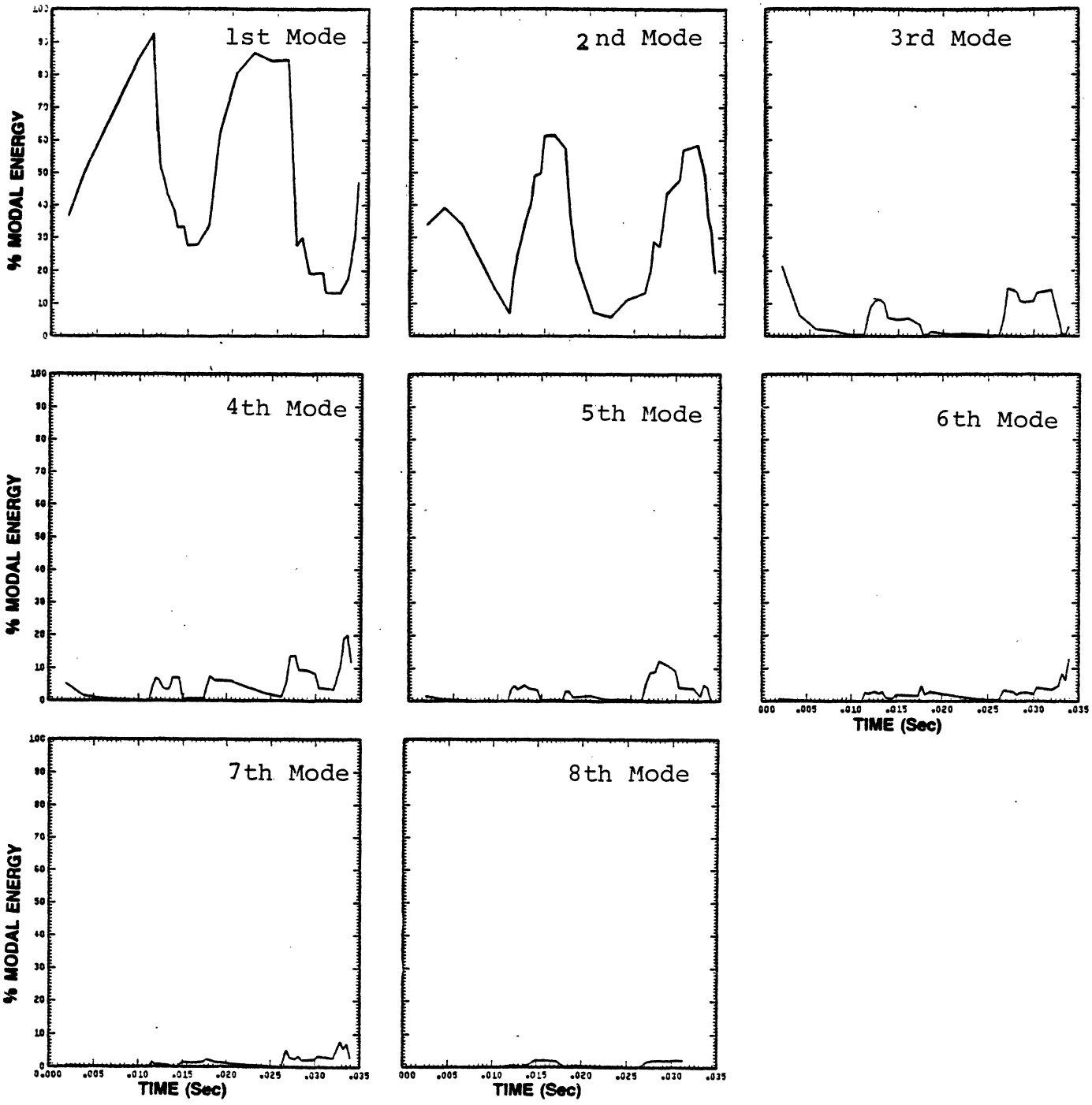

Figure 4.3 Percent modal energies of the cantilever beam.

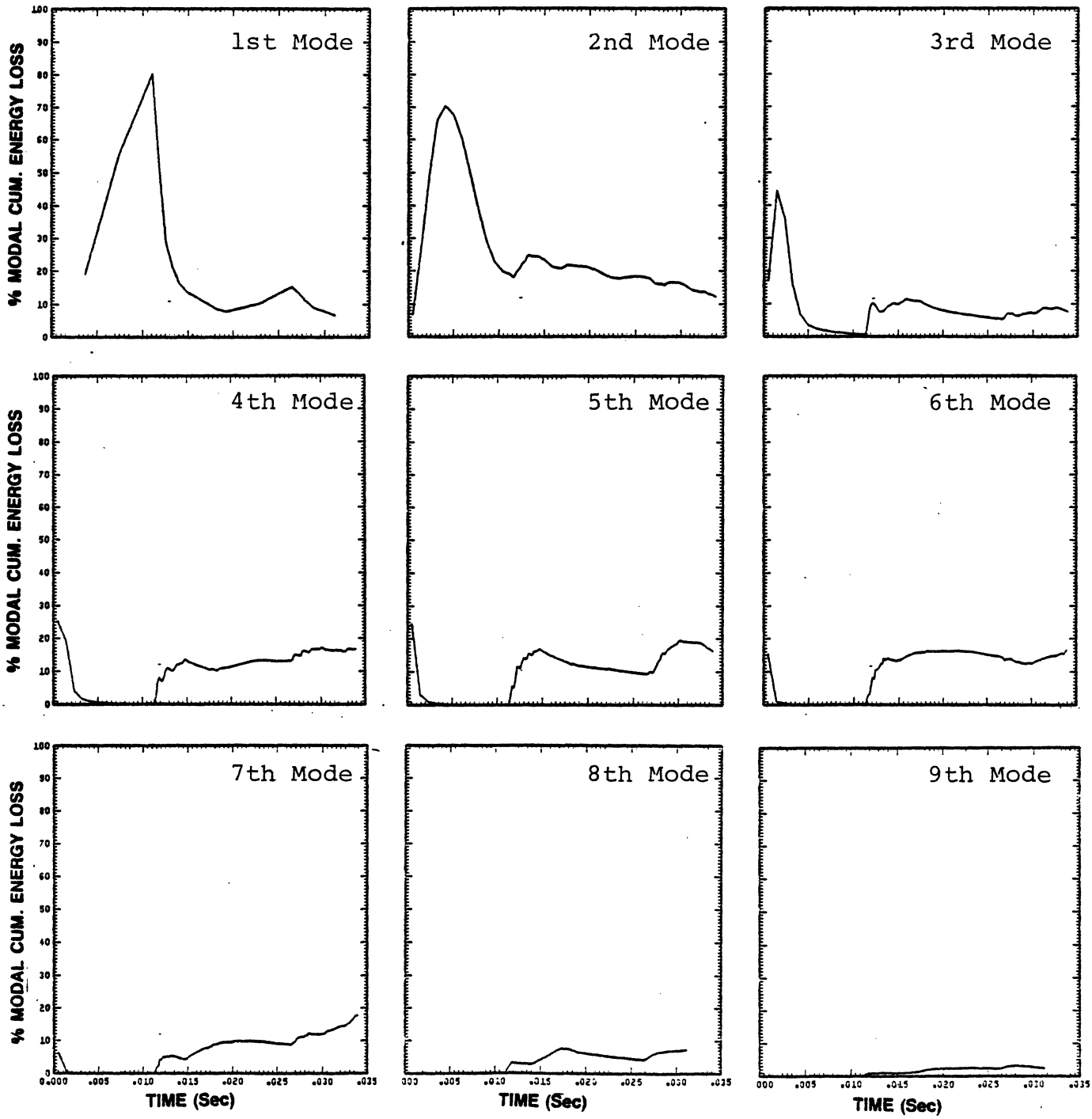

Figure 4.4 Percent modal cumulative energy losses of the cantilever beam.

impacting occurs. These figures also show the importance of the higher modes as energy dissipaters. Some higher modes are dissipating significant amounts of energy although their energy contents are not large. In this example, only the first 8 modes need to be taken into consideration. In general, the number of significant modes depend on the impact force level and the impact force durations. The higher the impact force, the greater the number of effective modes. As was discussed earlier, the support stiffness,clearance, and the excitation forcing function are the determining parameters.

In order to give some feeling for the system parameters and to see their effects on the results, the following runs were performed for the system given in Table 4.1. The results are tabulated in Tables 4.2 and 4.3. The variable parameters are,

(1) Coefficient of friction between the tube and the support

(2) Clearance

(3) Excitation forcing function

(4) Support stiffness

(5) Material damping of the support

One dimensional runs (Table 4.2) show the dependence of the RMS impact force on the excitation force amplitude, clearance, and support stiffness. From the results obtained, it can be seen that the RMS impact force increases with increasing clearance. When the clearance becomes large enough not to permit any impacting, the impact force sharply reduces to zero. Similiarly, the RMS impact force increases with increasing excitation force amplitude. Note that the relation between these two parameters becomes almost linear for the high excitation levels. The reason for this is that the displacement of the beam becomes significantly larger than the clearance and the system behaves as if there is no clearance. This makes the non-linear impacting problem an almost linear one for high excitation levels. The effect of the support stiffness does not appear to be a significant parameter as can be

Support Stiffness [N/m]	Clearance c_d [m]	Excitation force amplitude [N]	RMS Impact force [N]
2.0×10^6	2.5×10^{-3}	0.1	0.40
2.0×10^6	**5.0×10^{-3}**	0.1	0.42
2.0×10^6	**1.0×10^{-2}**	0.1	0.46
2.0×10^6	**1.6×10^{-2}**	0.1	0.64
2.0×10^5	$2.5 \times 10^{-}$	0.1	0.34
2.0×10^7	2.5×10^{-3}	0.1	0.65
2.0×10^6	2.5×10^{-3}	**0.02**	0.12
2.0×10^6	2.5×10^{-3}	**0.05**	0.18
2.0×10^6	2.5×10^{-3}	**0.15**	0.83
2.0×10^6	2.5×10^{-3}	**0.20**	1.30

Table 4.2 The effects of system parameters on the RMS impact force (1-dimensional runs)

seen in Table 4.2. When the support stiffness is increased 100 times, the resultant RMS impact force only increased by a factor of two.

For two dimensional runs, the cantilever beam is excited in both the y and z directions with the same sinusoidal forcing function as the one dimensional runs. Results are presented in Table 4.3. Calculated RMS impact forces are the same as the ones given in Table 4.2. In-plane displacements are defined to be the displacements in the plane where the flat bars do not provide any stiffness. Interestingly, none of the parameters seem to be effective in changing the steady-state in-plane displacements.

Support material damping changes the RMS impact force only a few percent and can be eliminated from the analysis. This is also reported by Rogers and Pick [8]. The effect of the phase angle, ϕ, is also investigated. There is a 90° phase difference between the streamwise and transverse excitation forces acting on a heat exchanger tube. Two separate runs with a 0° and a 90° phase angle produced almost the same result. In practice, it is not possible to center the tubes perfectly through the supports. Most of the time the tube rests on the support at a point. For such cases, computer simulation gives lower RMS impact forces, although the RMS displacements don't change much. This might be a good design tip to reduce the RMS impact force levels. On the other hand, the heat exchanger tube might fail in shorter time due to one sided wear, although the RMS impact force is smaller. In the case of one sided impact, the RMS impact forces at the supports on each side of the tube should be calculated separately. The largest of these forces should be compared with the RMS impact force on a perfectly centered tube. This test would show which arrangement results in longer tube life, because the smaller the RMS impact force, the longer the tube life.

The time step was allowed to vary in the above mentioned runs to save computing time. It was an intention of this study to obtain the frequency spectrum of the displacements so that the different mechanisms which might be important to the U-tube/flat bar support

Support Stiffness [N/m]	Clearance c_d [m]	Excitation force amplitude [N]	Coefficient of friction	S.S. in-plane displacement [m]
2.0×10^6	2.5×10^{-3}	0.1	0.1	1.25×10^{-3}
2.0×10^6	1.6×10^{-3}	0.1	0.1	1.23×10^{-3}
2.0×10^5	2.65×10^{-3}	0.1	0.1	1.30×10^{-3}
2.0×10^6	2.5×10^{-3}	0.02	0.1	2.5×10^{-3}
2.0×10^6	2.5×10^{-3}	0.1	0.0	1.30×10^{-3}

Table 4.3 The effects of the system parameters on the S.S. in-plane displacements (2-dimensional runs)

interaction could be investigated. Contact durations were not large enough to obtain sufficient frequency resolution in FFT. This ruled out the possibility of investigating individual impacts, and their frequency contents. Superposition of the data from the individual impacts did not give satisfactory results because of the discontiniuties. A small computer code was developed to obtain Fourier Transforms directly for varying time step. It worked well for a small number of points, but wasn't practical for use in runs using a large number of data points. Thus the data from the transient response computation was analysed using a Fast Fourier Transform (FFT) algorithm and the integration time step had to be held constant throughout the integration period. This meant that the computer runs were rather long and expensive. In reality, the heat exchanger tubes are excited by a wide-band random excitation function. In order to perform a random data analysis many runs and ensemble averaging of the results were necessary. Due to the high cost of the computer runs a deterministic excitation forcing function was chosen. The lowest three modes are excited simultaneously with a sinusoidal forcing function located at 45° from the U-bend apex (point A in Figure 2.11) and having identical magnitudes in the in-plane and the out-of-plane directions. The first of these modes corresponds to the lowest natural frequency (out-of-plane) and should be eliminated by the flat bar supports at the apex (point B in Figure 2.11). The dominant response should then be in the lowest in-plane mode and the second out-of-plane mode. Thus, the three most important modes for this investigation were excited at resonance. It is recognized that it would have been preferable to simulate the tube excitation by broad band random excitation distribution over the tube length. However, the cost of this approach would have been prohibitive as discussed above and it is felt that the excitation used represents a worst case.

4.2. ENERGY DISSIPATED BY THE HIGHER MODES

The U-tube shown in Table 4.4 was excited with the same forcing function in the in-plane and out-of-plane directions at its 3 lowest frequencies as discussed above. The physical parameters have the values presented in the same table. One percent critical damping was assumed for each mode. A six element FEM model was used to simulate the system. Calculated mode shapes and the natural frequencies are given in Figures 4.5-4.7 for the lowest three modes. Figures 4.8 and 4.9 show the resulting displacement-time and the impact force-time records respectively. It is seen that each major contact of the tube with a support is associated with a number of impacts. Figures 4.10 and 4.11 show the percent modal energies and the percent cummulative modal energy losses. In these figures only the modes with significant energy are shown, although the computations include 36 modes. As can be seen, the energy contents and the energy losses of the higher modes increase when tube/support impacting occurs. The odd numbered higher out-of-plane modes dissipate significant amounts of energy. These are the modes with an anti-nodal point at the apex, as is the first out-of-plane mode which should be restrained and/or excited by the flat bar supports. Note that the most significant mode in terms of energy content after a number of impacts is the second out-of-plane mode which is being excited at its antinode and has the supports at its nodal point. At 0.15 seconds, this mode contains over 70% of the modal energy, but its cumulative contribution to the energy loss is less than 25%. Note as well that only the first two in-plane modes are significant and that the effect of impacting at the supports tends to reduce their percentage contributions in time. This observation is particularly significant if the first in-plane mode is being excited at resonance by a force with a component in the in-plane direction. The first in-plane mode does not contain as much energy as the second out-of-plane mode, although it has a lower natural frequency than the apparently dominant second out-of-plane mode. The reason is that the second out-of-plane mode was excited at its

Fixed Parameters

$E = 2.3 \times 10^{11}$ [N/m]

$\nu = 0.3$

$\rho_{sur} = 1.26$ [kg/m^3]

$\rho_b = 7920.0$ [kg/m^3]

$k_{sp} = 2.0 \times 10^6$ [N/m]

$d_i = 0.01003$ [m]

$d_o = 0.0158$ [m]

$\alpha = 0.25$ [sec/m]

$\Delta t = 1/35000$ [sec]

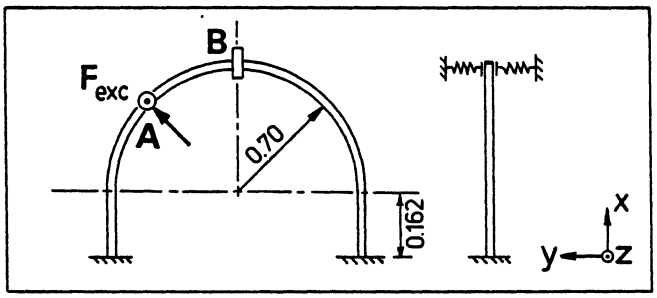

$F_{exc}(t) = F_{max}(\sin(2\pi f_1 t) + \sin(2\pi f_2 t) + \sin(2\pi f_3 t))$

Reference Values of the Varying Parameters

$\mu = 0.20$

$c_d = 2.5 \times 10^{-4}$ [m]

$F_{max} = 0.1$ [N]

Table 4.4 The system parameters of the U-tube

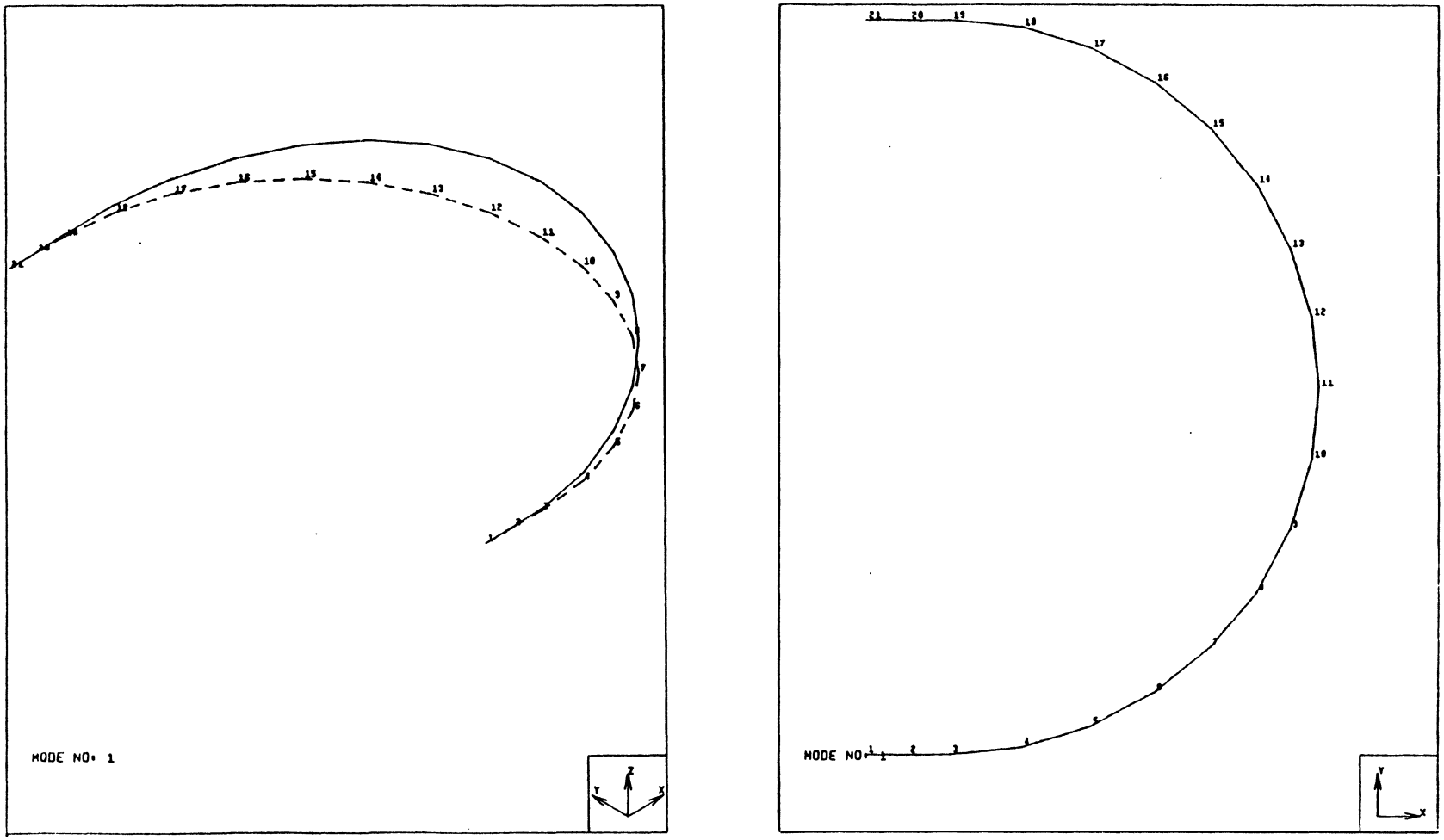

Figure 4.5 Mode shape of the first out-of-plane mode.

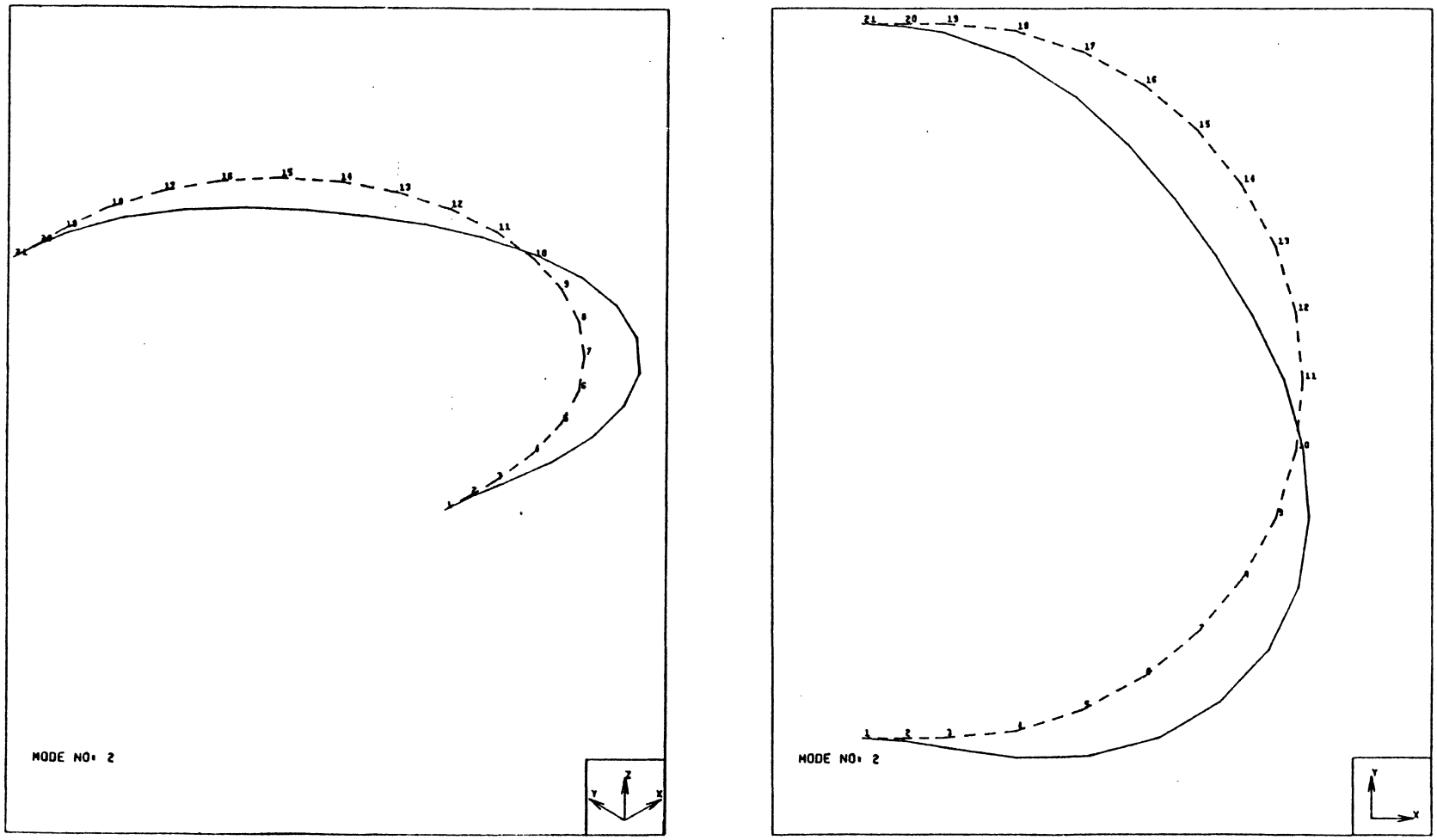

Figure 4.6 Mode shape of the first in-plane mode.

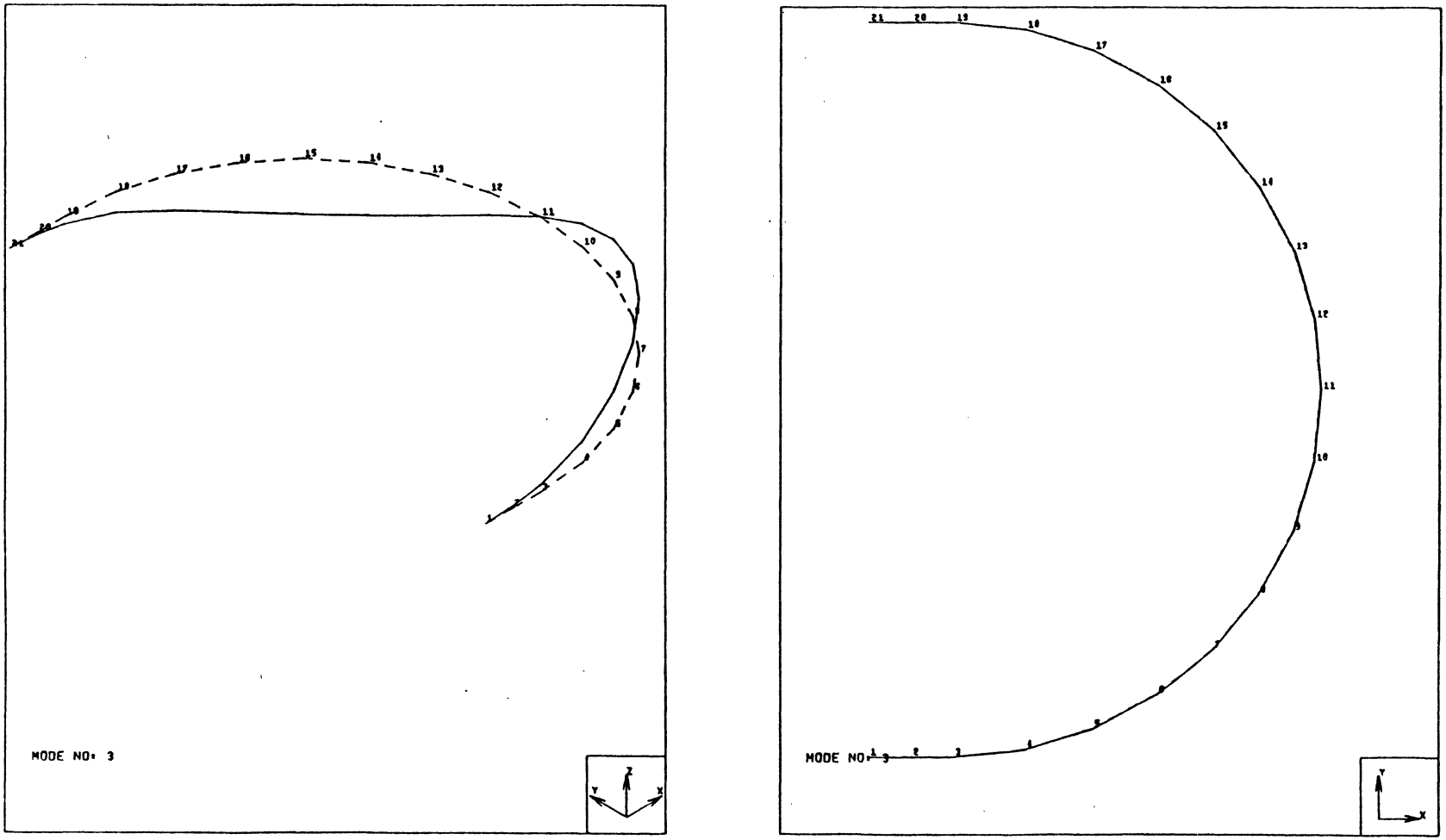

Figure 4.7 Mode shape of the second out-of-plane mode.

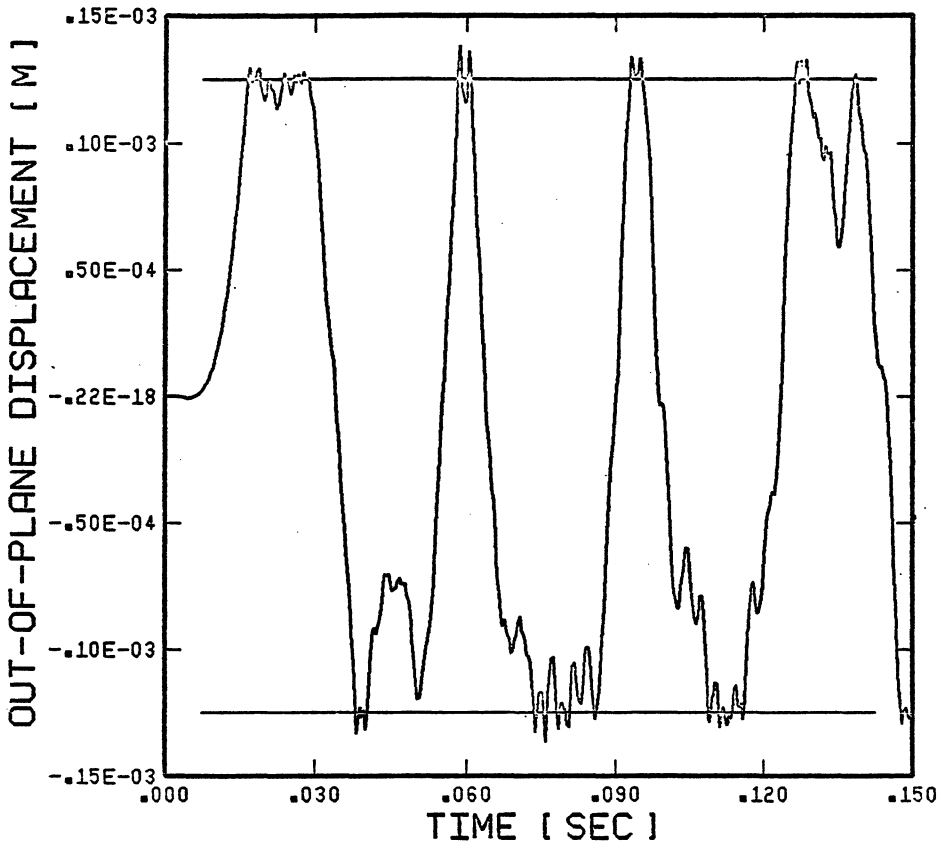

Figure 4.8 Displacement history of the U-tube at the apex.

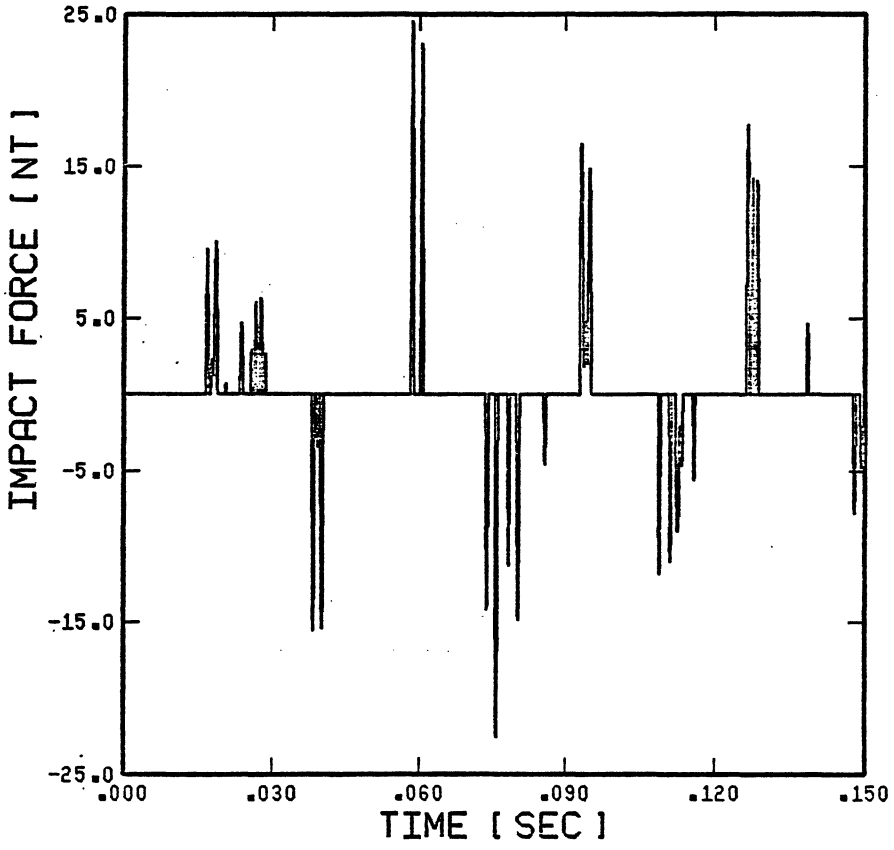

Figure 4.9. Impact force history of the U-tube with flat bar supports.

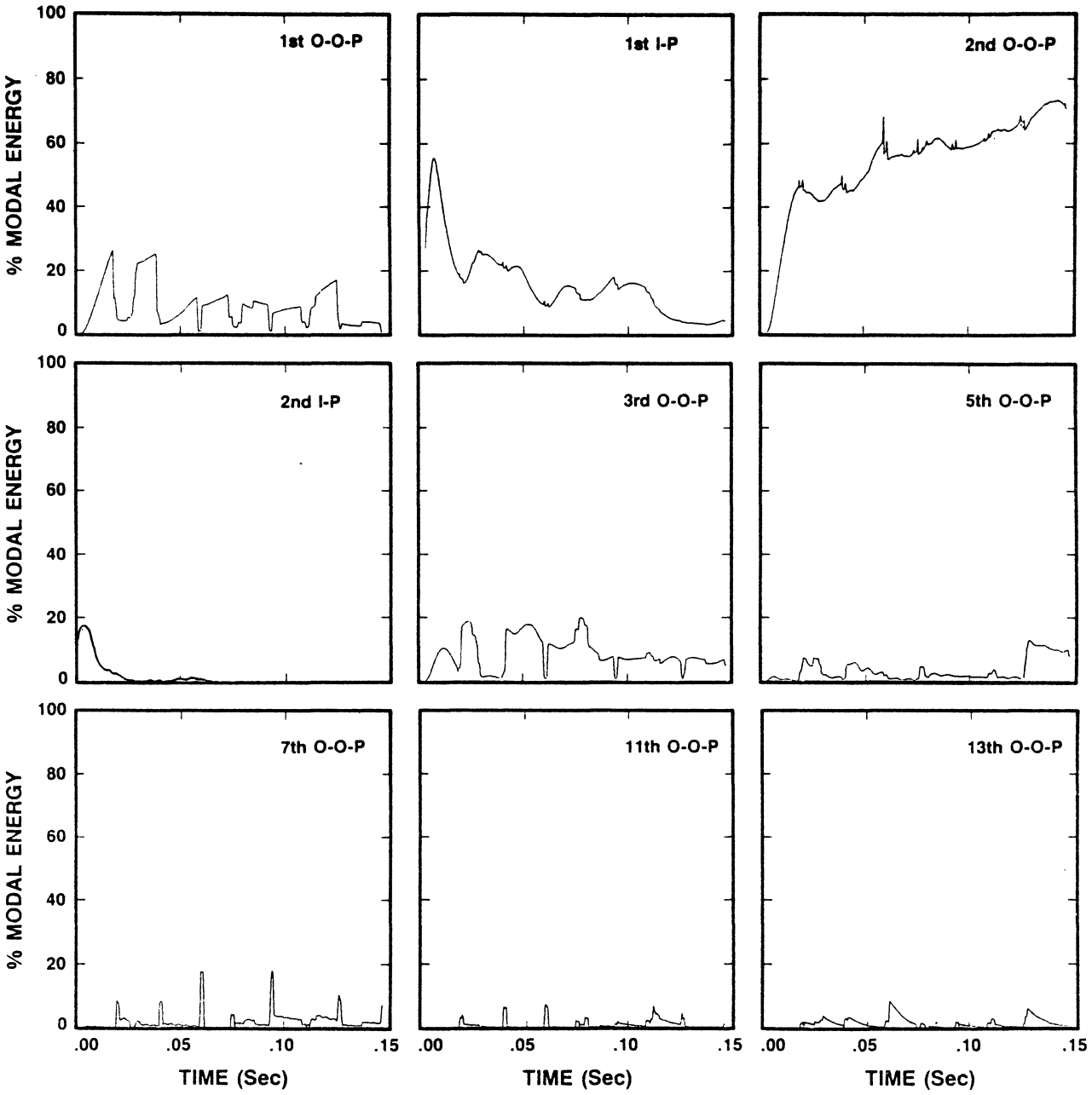

Figure 4.10 Percent modal energies of the U-tube.

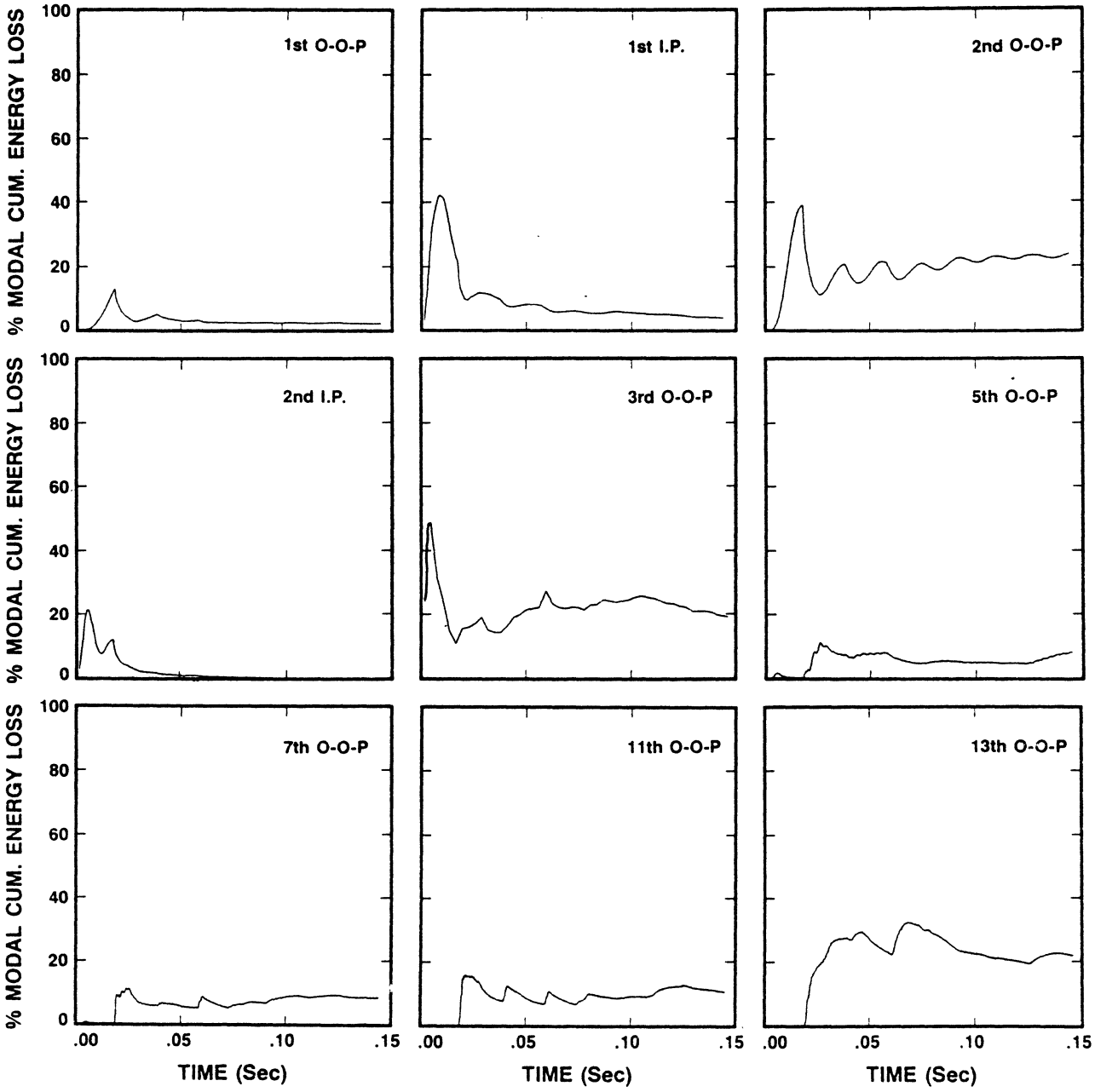

Figure 4.11 Percent modal cumulative energy losses of the U-tube.

antinode, but the first in-plane mode was not. Also, the first in-plane displacement is damped by friction at the support location which is the antinode of the first in-plane mode.

The number of significant modes in energy dissipation depends on the impact force level and the contact time. The higher the impact force and the shorter the contact time, the greater the number of significant modes. Since the following parameters determine the impact force levels and the contact durations, they also determine the number of significant modes. These parameters are: support stiffness, clearance, and the excitation forcing function. In general most of the energy dissipation occurs in the lowest modes, although some higher modes make a significant contribution. It should be noted that if the damping factors in the higher modes were reduced as would be likely in practical heat exchangers, the energy dissipation in these modes would be even less.

4.3 THE EFFECT OF INCREASING EXCITATION FORCE LEVELS

In order to investigate the effect of support impacting and the mode coupling on the U-tube response, the excitation force levels were varied. From the results obtained, three different regimes were distinguished : (1) low excitation levels, (2) moderate excitation levels, and (3) high excitation levels. There is no tube-support impacting for the case of low excitation levels (as in Figure 4.12(a)). The system behaves linearly and as if no support existed. This is what Chen et al. [13] call a "tube support inactive mode". The frequency spectrum changes when impacting occurs. In the case of moderate excitation levels (Figures 4.12(b) and 4.12(c)), the tube contacts the support occasionally. The system is non-linear, and therefore the relative modal contributions are strongly dependent on the excitation level. The flat bar supports significantly reduce the first out-of-plane response as expected (Figures 4.12(b)-(d)) as the excitation levels increase. Impacting is regular in the case of high excitation levels and the first out-of-plane response is effectively eliminated. Note also the

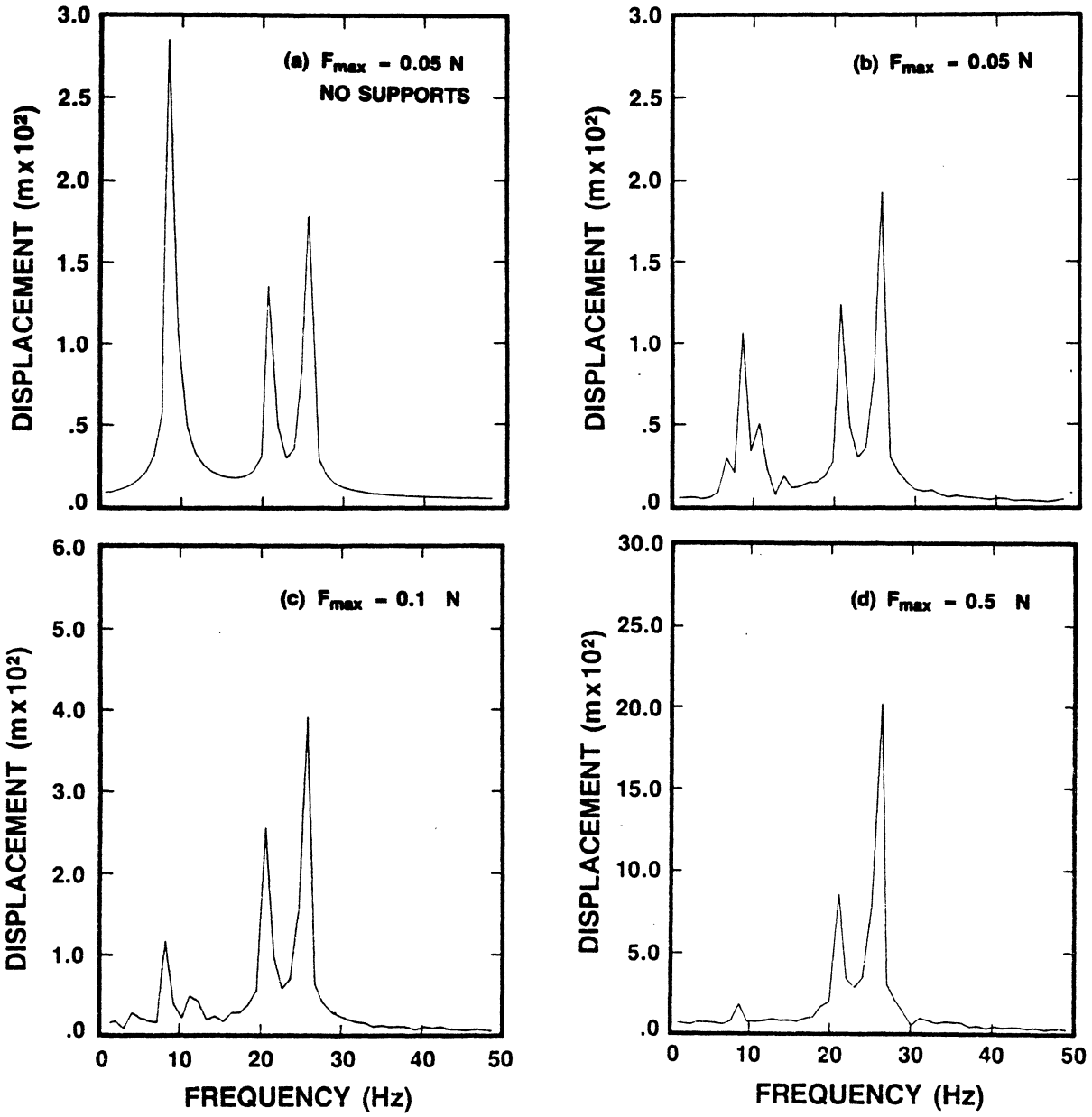

Figure 4.12 The effect of increasing excitation level.

reduction in amplitude of the first in-plane mode due to friction at the supports. The system again behaves like a linear one, the second out-of-plane amplitude increasing linearly with the excitation level (Figure 4.12(d)). These results are essentially in agreement with the experiments of Chen et al. [13].

The displacement values in Figure 4.12 were taken at the point of excitation and used to compute the response spectrum using an FFT algorithm. Since this point is the antinode of the second out-of-plane mode but not the antinode of the first in-plane mode, the second out-of-plane mode peak (27 Hz) is larger than the first in-plane mode peak (21 Hz) in Figure 4.12(a). The second out-of-plane mode is unaffected by the changing excitation force levels since the support, and hence the impact force included in the analysis, is at the apex and this is the nodal point of the second out-of-plane mode. The first in-plane mode peak is smaller in Figures 4.12(b) and 4.12(c) than in Figure 4.12(a). This is due to the friction damping which increases with the excitation level. This peak gets even smaller for high excitation levels because the RMS impact force levels are much higher. Note that the vertical scales in Figure 4.12(a)-(d) have been changed linearly with increasing excitation force levels for ease of comparison of response levels.

4.4 THE EFFECT OF MODE COUPLING

The in-plane and out-of-plane modes are coupled by means of the friction force at the supports as explained in section 2.2.8. To investigate this coupling, the U-tube was excited using the same moderate level forcing function used above. Three different coefficients of friction, 0.0, 0.2, and 0.4, were used for three separate computer runs and the results are summarized in Figure 4.13. The change in the coefficient of friction has a negligible effect on the second out-of-plane mode as expressed. The first in-plane mode response reduces as the friction coefficient increases. This is also expected because friction

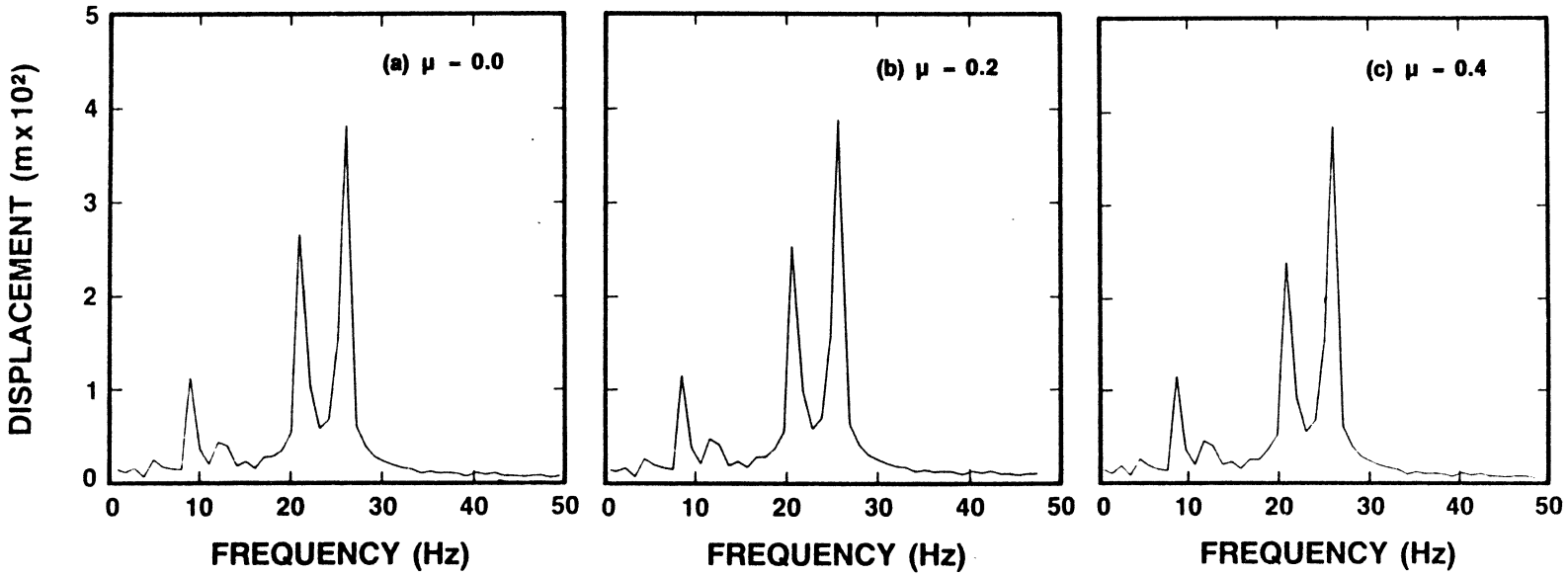

Figure 4.13 The effect of mode coupling by means of friction.

force always opposes the motion. The peak corresponding to the first in-plane mode is 5.8% and 11.2% less in Figures 4.13(b) and 4.13(c) than that shown in Figure 4.13(a). These results suggest an almost linear relationship between the in-plane displacements and the coefficient of friction for a fixed excitation level.

For the U-bend tube under study, the flat bar supports are in the plane of the U-bend and the TQ_i term is zero in Equation 2.25. Equations 2.25 and 2.26 are uncoupled when the friction coefficient is zero, because f_{spr} and f_{dmp} are functions of out-of-plane displacements only and f_f and TQ_o are both zero. The friction force, f_f, does have some effect on the in-plane motion in the form of friction damping (Figures 4.13(a)-(c)). However, the important result is that friction does not cause significant coupling of the in-plane and out-of-plane modes.

4.5 THE EFFECT OF CLEARANCE

The change in clearance has a negligible effect on the first in-plane and the second out-of-plane modes as shown in Figure 4.14. However, it does affect the first out-of-plane mode in a way similar to the excitation level. Doubling the clearance (Figure 4.14(b)) produces results similar to halving the excitation level (Figure 4.14(b)). It is also interesting to note that the RMS impact forces increased only 5% although the clearance changed by a factor of two. This is in agreement with the findings of Axisa et al. [12].

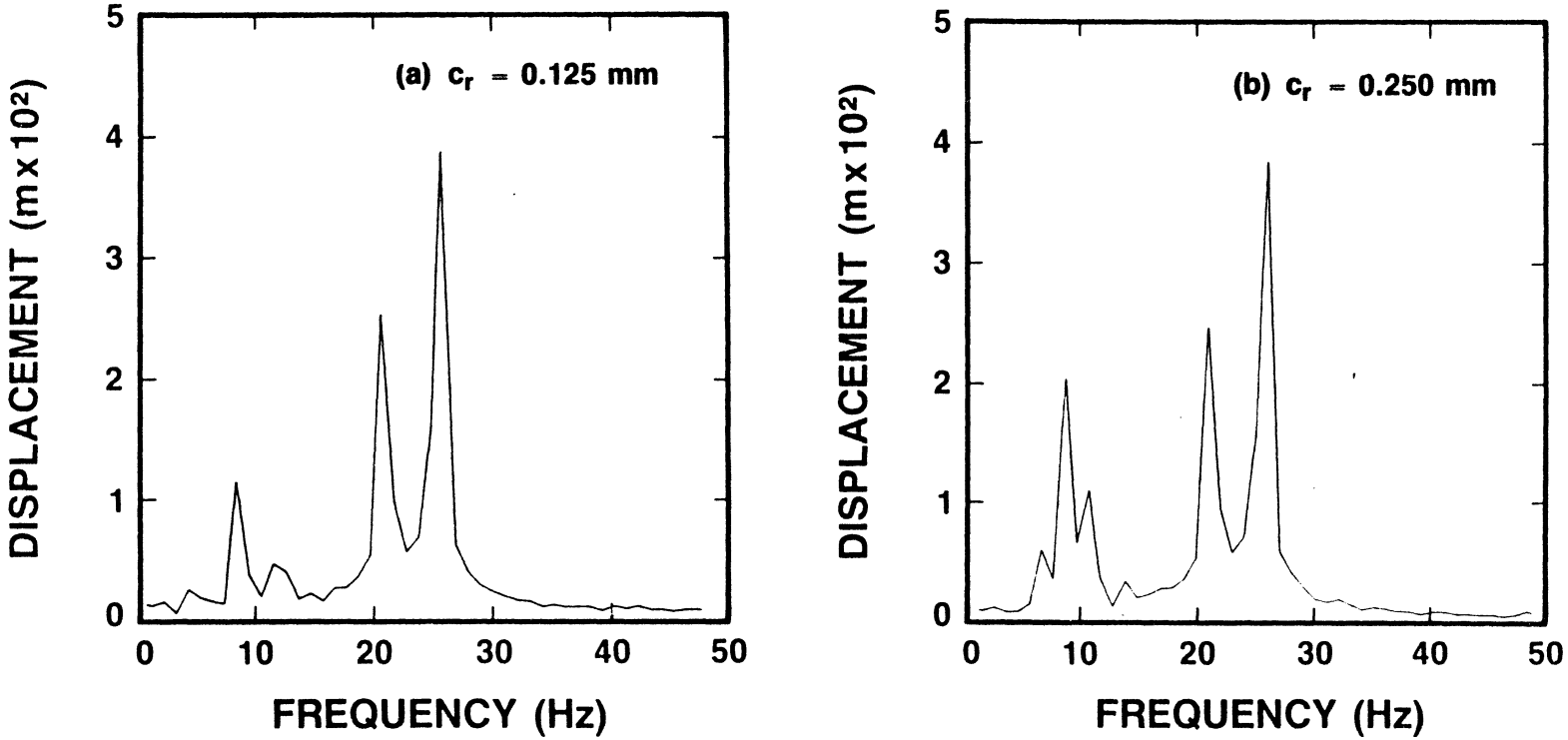

Figure 4.14 The effect of clearance.

CHAPTER 5

CONCLUSIONS

The results obtained from this theoretical analysis of the response of a U-tube with flat bar supports at its apex suggest the following :

(1) Although some of the energy is transfered to higher modes due to impacting, most of the energy is dissipated by the lower modes. The contribution of the higher modes to the total displacement is negligible.

(2) The predicted response essentially agrees with in the experiments of the previous studies. At low excitation levels, there is no impact and all free modes are observed. As the excitation levels are increased, the response is nonlinear and the tube support impacting reduces the response in the restrained modes. Higher odd numbered out-of-plane modes (the modes with an antinode at the support the same as the restrained first out-of-plane mode) are excited with the impact force. At high excitation levels, the response in the restrained first out-of-plane mode effectively disappears and the system behaves almost linearly.

(3) Mode coupling by means of friction has some effect on the in-plane displacements and negligible effect on the out-of-plane displacements. The in-plane displacement decreased approximately linearly as the coefficient of friction was increased. In the case of instability, these effects of mode coupling might be amplified.

(4) The effect of clearance on the RMS impact force level is very small, probably because of the reduced number of impacts. The change in

clearance affects the first out-of-plane mode in a similar way to the change in excitation level.

(5) A new approach, the stiffness method, produces more accurate and cost efficient results for single support impact problems. However, the previously used external force method is more flexible for the systems with multi-supports and more importantly, it permits the use of modal analysis.

CHAPTER 6

RECOMMENDATIONS

The present study provided more insight into the understanding of the dynamic characteristics of the flat bar supports and the behaviour of the tube-support impacting. A sinusoidal excitation force was applied on the system. In practice the nature of the dominant excitation has been known to be the broad-band random excitation. Random forces due to turbulence can be simulated by using a random number generator. However, ensemble averaging would be necessary in the case of randomness and this would increase the computing cost considerably. The sinusoidal forcing function is thought to be a worst case and the results arevalid for the purpose of this study.

The nature of the structural damping induced due to tube-support impacting has not been investigated and the available data is highly scattered. Since the damping significantly affects the tube behaviour, more serious work is necessary to model the damping properly.

Since a forced excitation was applied to the system, the results obtained were all in the stable range. Although the results were in good agreement with previous experiments [2], the questions concerning the stability threshold and post-stable behaviour remain unanswered. The fluid-structure interaction is necessary for instability and the behaviour of the system might be significantly different at the stability threshold. Therefore, a fluidelastic model which includes the mutual interaction of the structure and the fluid is needed to investigate the behaviour of the heat exchanger tubes at the stability threshold and in the post-stable range. The effectiveness of the flat bars can be better understood with such an analysis. This might be accomplished by combining a beam finite element program and a fluid flow finite element program. However, present day computer solutions of Navier-Stokes

equations are possible only for very low Reynolds number flows which are out of the practical range of flow induced vibrations. Simulation of the moving boundaries due to the vibrating tube would also increase the computing cost. On the other hand, present day simplified analytical solutions [27] that can predict the unsteady fluid force coefficients on heat exchanger tubes still need to be improved.

Due to the limitations in theoretical solutions, in order to explain the effectiveness of the flat bars on U-bend tubes and the effect of the U-tube curvature experimental work is needed. It is probable that the stability threshold for the curved tubes is higher than for the straight tubes, for it will be comparatively harder to form a regular flow periodicity and mutual interaction because of the asymmetric geometry and stiffness.

More experimental work based on Weaver and Schneider's experiments [2], would explain why the flat bar supports are effective in in-plane directions. First of all, an investigation should be instigated to determine if the curved tubes would go unstable in the absence of friction in in-plane directions. It is the friction that couples the in-plane modes with the out-of-plane modes and imposes friction damping in in-plane directions if the fluid excitation is forced. In the case of forced excitation and no friction, the governing equations of motion given in section 2.2.8 predict an instability in the in-plane directions once the lowest out-of-plane mode is eliminated. This can be investigated by repeating Weaver and Schneider's experiments [2] using piano wires to restrict out-of-plane motion instead of flat bars. Piano wires would eliminate the first out-of-plane mode and wouldn't impose any friction in in-plane directions.

If there is no in-plane instability observed with piano wires, then it is not the friction that keeps the U-tube stable in in-plane directions. In this case it would be the effect of curvature that would effect the mutual interaction of the U-tubes and the fluid would keep the U-tubes stable in in-plane directions.

If in-plane instability is observed with the piano wires, then it is the friction force which is responsible for in-plane stability. In this case it would be useful to determine the change in the in-plane stability threshold with the changing coefficient of friction. By using lubricants and/or reducing the flat bar support areas it is possible to reduce the friction. The expected behaviour patterns for this case are as follows. When the friction coefficient is small, the U-tubes will go unstable in the lowest in-plane mode. In the limiting case when the coefficient of friction is zero, the behaviour will be the same as the one with piano wires. When the coefficient of friction increases, the combined effect of in-plane friction damping and in-plane/out-of-plane mode coupling would delay the instability. Through a set of experiments mentioned above, the level of friction necessary to prevent in-plane instability can be obtained.

REFERENCES

[1] PAIDOUSSIS M.P., "Flow Induced Vibration of Cylindrical Structures : A Review of the State of Art", MERL Report 82-1 (1982)

[2] WEAVER D.S., SCHNEIDER W., "The Effect of Flat Bar Supports on the Cross flow Induced Response of Heat Exchanger U-Tubes", ASME Paper 82-JPGC-NE-12 (1982)

[3] CHEN S.S., ROSENBERG G.S., WAMBSGANSS M.W., "On Tube Baffle Impact During Heat Exchanger Tube Vibration", Symp. on Flow Induced Vibration in Heat Exchangers, Winter Annual Meeting of ASME, New York, 27-35 (1970)

[4] TING E.C., CHEN S.S., WAMBSGANSS M.W., "Dynamics of Component/Support Impact : An Elastic Analysis ", ANL-CT-78-31, Argonne National Laboratory (1978)

[5] WATANABE T., "Steady Impact Vibration of Continious Elements", Bulletin of the JSME, v24, 222-228 (1981)

[6] BOHM G.J., NAHAVANDI A.N., "Dynamic Respose of Reactor Internal Structures with Impact Between Components", Nucl. Sci. Eng., v47, 391-408(1972)

[7] ELLIOT G.L., "Dynamic Response of Heat Exchanger Tubes", M.Eng Thesis, University of Waterloo, Waterloo, Ontario (1973)

[8] ROGERS R.J., PICK R.J, "On the Dynamic Spatial Response of a Heat Exchanger Tube with intermittent Baffle Contacts", Nucl. Eng. Design, 81-90 (1976)

[9] SHIN Y.S., JENDRZEJCZYK J.A., "Effect of Tube/Support Interaction on the Vibration of a Tube on Multiple Supports", ANL-CT-77-5, Argonne National Laboratory (1977)

[10] SHIN Y.S., SASS D.E, JENDRZEJCZYK J.A., "Vibro-Impact Responses of Tube with Tube-Baffle Interaction", Trans. of the CSME, v5, n1, 15-23 (1978)

[11] HASLINGER K.H. AND STEININGER D.A., "Steam Generator Tube/Tube Support Plate Interaction Characteristics", Symposium on Flow-Induced Vibration, Winter Annual Meeting of ASME, New Orleans, v3, 45-62 (1984)

[12] AXISA F., DESSEAUX A., AND GIBERT R.J., " Experimental Study of Tube/ Support Impact Forces in Multi-Span PWR Steam Generator Tubes", Symposium on Flow-Induced Vibration, Winter Annual Meeting of ASME, New Orleans, v3, 139-148 (1984)

[13] CHEN S.S., JENDRZEJCZYK J.A. AND WAMBSGANSS M.W., "Dynamics of Tubes in Fluid with Tube-Baffle Interaction", Symposium on Flow-Induced Vibration, Winter Annual Meeting of ASME, New Orleans, v2, 285-304 (1984)

[14] KO P.L., "Experimental Studies of Tube Fretting in Steam Generators and Heat Exchangers", ASME J.Pressure Vessel Technology, v101, 125-133 (1979)

[15] PETTIGREW M.J., KO P.L., "A Comprehensive Approach to Avoid Vibration and Fretting in Shell and Tube Heat Exchangers", ASME Publ., Flow Induced Vibration of Power Plant Components, PVP-41, 1-18 (1980)

[16] BLEVINS R.D., "Fretting Wear of Heat Exchanger Tubes, Part 1 : Experiments ", J. Eng. for Power, v101, 625-629 (1979)

[17] BLEVINS R.D., "Flow Induced Vibration", Van Nostrand Reinhold Company (1977)

[18] THOMAS D.L., WILSON J.M., WILSON R.R, "Timoshenko Beam Finite Elements", J. Sound and Vibration, v31, 315-330 (1973)

[19] PRZEMIENIECKI J.S., "Theory of Matrix Structural Analysis", McGraw Hill Book Company (1967)

[20] BELYTSCHKO T., "A Survey of Numerical Methods and Computer Programs for Dynamic Structural Analysis", Nucl. Eng. and Desg., v37, 23-34 (1976)

[21] KREIG R.D., KEY S.W., "Transient Shell Response by Numerical Time Integration", Int. J. for Num. Meth. in Eng., v7, 273-286 (1973)

[22] COWPER G.R., "The Shear Coefficient in Timoshenko's Beam Theory", ASME J. Appl. Mech., 81-90, (1966)

[23] ENGEL P.A., "Impact Wear of Materials", Elsevier Scientific Book Company, Amsterdam (1975)

[24] PETTIGREW M.J., SYLVESTRE Y., CAMPAGNA A.O., "Vibration Analysis of Heat Exchanger and Steam Generator Designs", Nucl. Sci. and Desg., v48, 97-115 (1978)

[25] BATHE K.J., WILSON E.L., "Numerical Methods in Finite Element Analysis", Prentice Hall (1976)

[26] ZIENKIEWICZ, O., The Finite Element Method, 3rd Edition, McGraw Hill (1977)

[27] LEVER, J.H. and WEAVER, D.S., "On the Stability Behaviour of Heat Exchanger Tube Bundles. Part 1 - Modified Theoretical Model", ASME Symposium on Flow Induced Vibrations, V2, New Orleans, 83-98 (1984)